Journal of Membrane Science & Research

journal homepage: www.msrjournal.com

Research Paper

Mixed Matrix Membranes from Polyetherimide: Development, Characterization, and Applications in Pervaporation and Gas Separation

Greeshma Thankachan [1], Mariia Dmitrenko [2], Anna Kuzminova [2], Roman Dubovenko [2], Usha K. Aravind [1], Charuvila T. Aravindakumar [3], Maxim Shalygin [4], Lyudmila Gasanova [4], Anastasia Penkova [2,*]

[1] *School of Environmental Studies, Cochin University of Science and Technology, Cochin, 682022, Kerala, India*
[2] *St. Petersburg State University, 7/9 Universitetskaya nab., St. Petersburg 199034, Russia*
[3] *School of Environmental Sciences, Mahatma Gandhi University, Kottayam, 686560, Kerala, India*
[4] *A.V. Topchiev Institute of Petrochemical Synthesis, Russian Academy of Sciences, 29 Leninskiy prospect, Moscow, 19991, Russia*

Article info

Received 2025-08-28
Revised 2025-12-06
Accepted 2025-12-14
Available online 2025-12-14

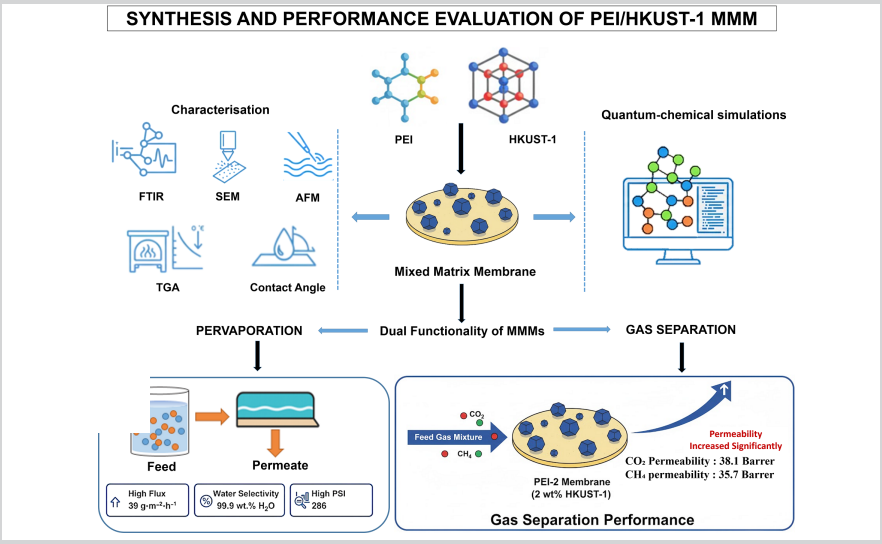
Keywords

Polyetherimide
Metal-Organic Framework
Mixed Matrix Membranes
Pervaporation
Gas Separation

Highlights

- Developed PEI/HKUST-1 mixed matrix membranes for both pervaporation and gas separation.
- Tests with ATR-FTIR, SEM, AFM, TGA, and contact angle showed the MOF was well incorporated, improving structure, hydrophilicity, and thermal stability.
- The best membrane, with 2 wt.% HKUST-1, gave 39 $g \cdot m^{-2} \cdot h^{-1}$ flux, PSI of 286, and 99.9 wt.% water selectivity in separating water/isopropanol.
- CO_2 and CH_4 permeability was improved greatly over pure PEI, and computer simulations helped explain how molecules moved and interacted inside the membranes.

Graphical abstract



Abstract

Mixed matrix membranes (MMMs) based on polyetherimide (PEI) and the Cu-based metal-organic framework (MOF) HKUST-1 were fabricated and comprehensively evaluated for dual functionality in gas separation and pervaporation applications. Structural and physicochemical characterization confirmed the incorporation of HKUST-1, leading to significant changes in internal morphology, surface roughness, hydrophilicity, and thermal stability. Quantum-chemical simulations were employed to predict and interpret transport behavior and molecular interactions within the composite system. Among the prepared membranes, the PEI/HKUST-1 membrane containing 2 wt.% MOF exhibited optimal performance in pervaporation, achieving a high permeation flux of 39 $g \cdot m^{-2} \cdot h^{-1}$, a pervaporation separation index of 286, and exceptional water selectivity (99.9 wt.%) during the separation of an azeotropic water/isopropanol mixture. Temperature-dependent studies further confirmed the membrane's operational stability and efficiency. In gas separation, the same membrane demonstrated significantly enhanced CO_2 and CH_4 permeability compared to the unmodified PEI membrane. These results highlight the potential of PEI/HKUST-1 MMMs as promising and multifunctional materials for advanced membrane-based separation technologies.

© 2026 FIMTEC & MPRL. All rights reserved.

* Corresponding author: a.penkova@spbu.ru (A. Penkova)

DOI: 10.22079/jmsr.2025.2070180.1725

1. Introduction

Membrane technology provides energy-efficient substitutes for traditional methods like absorption and distillation. It has emerged as a major component of sustainable separation processes in energy, chemical, and environmental applications [1,2]. Mostly in azeotropic systems, such as gas separation and pervaporation, have become important solutions for important problems, including solvent dehydration, carbon capture, and natural gas purification [3,4].

Using selective sorption and vacuum-driven evaporation to overcome azeotropic constraints without entrainers, pervaporation is especially effective for dehydrating organic solvents (such as ethanol, isopropanol, etc.) [5]. According to recent studies, it can remove up to 99.5% of the water from azeotropic alcohol mixtures [6,7], while using 40% less energy than extractive distillation [8,9]. Similar to this, gas separation technologies are essential for industrial gas purification [10,11], CO_2 collection [12,13], and natural gas processing [14,15]. These membrane technologies offer significant benefits over traditional techniques, such as energy efficiency, environmental friendliness, compactness, and lower operating costs [16,17]. However, the intrinsic trade-off between permeability and selectivity, as well as the instability of membranes under demanding operating conditions, continues to restrict their industrial use [18].

The development of more effective membrane materials that combine high performance, durability, and processability remains the main goal of membrane technology to address these problems [19,20]. Although inorganic/ceramic membranes are very resistant to heat and chemicals, their high cost and fragility prevent them from being commercially scalable [19–21]. Cellulose acetate, polyimide, polysulfone, polyvinylidene fluoride, polydimethylsiloxane, polyvinyl alcohol, polyelectrolyte complex, polyamide, and polyether-block-amide in pervaporation [20] and gas separation [21] are important materials for polymeric membranes because of their tunable properties and affordability. Among these, polyetherimide (PEI) stands out as a particularly versatile choice that addresses significant shortcomings of conventional polymers by balancing strong mechanical/thermal properties, chemical resistance, and adaptability for both solvent dehydration and gas separation (such as CO_2/N_2) [22–24].

PEI is a strong engineering thermoplastic that is popular for membrane manufacturing due to its exceptional film-forming qualities, high heat resistance, and superior mechanical strength [25]. The glass transition temperature and intrinsic selectivity for gas separation are two important features that make PEI a great option. However, due to its intrinsically limited gas permeability, it suffers from the conventional permeability-selectivity trade-off and low resilience to plasticization under challenging working conditions in pervaporation applications [26,27]. The development of mixed matrix membranes (MMMs) has attracted attention as a solution to these limitations. This technique combines the superior sorption and diffusional properties of inorganic materials with the mechanical and processing benefits of polymers by inserting fillers into polymer matrices [28,29]. Graphene oxide (GO) and layered perovskite oxides are among the fillers that have been investigated. For instance, Pulyalina and associates discovered that when layered perovskite oxide ($La_{0.85}Yb_{0.15}AlO_3$) was added to PEI-based membranes, the permeation flux during the separation of methanol and cyclohexane increased, but the selectivity was slightly reduced. In contrast, this filler improved selectivity for O_2/N_2 and He/N_2 gas pairings while decreasing permeability for gas separation [23]. Furthermore, studies [24,30] have shown that incorporating GO into PEI membranes can enhance the separation efficiency of water/butanol and diethyl phthalate/water combinations, respectively.

Metal-organic frameworks (MOFs) are widely recognized as promising fillers for MMMs[5,31]. Their high surface area, tunable pore structure, and strong compatibility with polymer matrices (enabled by ligand-polymer interactions) make them highly attractive for membrane applications [2,6,27,32]. Additionally, their selective adsorption properties further enhance separation performance. In this regard, HKUST-1, a highly studied MOF based on copper, $Cu_3(BTC)_2$, has shown excellent compatibility with polymer matrices, a large surface area, a high capacity for CO_2 adsorption, and thermal stability up to 300 °C [33–36]. These properties make it particularly suitable for enhancing gas transport and sorption selectivity in polymer matrices [36]. Moreover, the presence of open metal sites and hydrophilic pores makes HKUST-1 an excellent filler candidate for water-selective pervaporation membranes. As demonstrated by [33], strong specific interactions between water molecules and the hydrophilic $Cu_3(BTC)_2$, along with preferential water transport pathways through HKUST-1 and associated morphological changes, led to a 1.8-fold increase in permeation flux while reducing the separation factor from 250 to 210 for the separation of water/ethanol mixtures. Furthermore, HKUST-1 shows significant potential for the separation of water/isopropanol mixtures, as its pore dimensions enable molecular sieving by being larger than a water molecule (~3 Å) yet smaller than an isopropanol molecule (~16 Å) [4,37]. Notably, HKUST-1 has also shown remarkable potential for hydrogen separation applications. Wang et al. [25] reported that incorporating 30 wt.% nanocrystals (50-80 nm) of HKUST-1 into a PEI matrix achieved exceptional gas separation performance, with hydrogen permeability reaching 193.3 Barrer and selectivity values of 20.6 for H_2/CO_2 and 101.7 for H_2/CH_4. This enhancement was attributed to three synergistic effects: (1) increased free volume, (2) creation of additional molecular transport pathways, and (3) improved selective sorption resulting from reduced interface defects. Thus, all these effects synergistically lead to increased permeability and selectivity in both gas separation and pervaporation applications, successfully resolving the limits of pure PEI membranes [38]. Moreover, despite the demonstrated advantages of MMMs based on PEI, the number of effective modifiers for PEI reported in the literature remains restricted. Challenges such as particle agglomeration, interfacial voids, and compatibility between the filler and polymer phase remain significant hurdles that might contribute to performance decline [25]. Based on existing literature, no research has comprehensively studied PEI-based MMMs modified with micro-sized HKUST-1 for both the pervaporation dehydration and the biogas separation of a CO_2/CH_4 mixture. To the best of our knowledge, there are no existing studies in the literature investigating membranes based on PEI modified with HKUST-1 for pervaporation dehydration.

The novelty of this work lies in the first complete investigation of how the inclusion of a micro-sized modifier, HKUST-1, into the PEI matrix changes its structure and transport capabilities in diffusion membrane processes. Additionally, it showcases the creation of a high-performance, multipurpose membrane from PEI/HKUST-1 composite designed for both gas separation and pervaporation applications that is extremely pertinent and promising in the ongoing search for reusable and adaptable membrane technologies. The polymer matrix was mixed with a range of HKUST-1 loadings (0-5 wt.%). At various filler concentrations, the membranes' suitability for both separation procedures was assessed. To understand the structural and physicochemical characteristics of the membranes, thorough characterization was used, including Attenuated Total Reflectance Fourier transform infrared spectroscopy (ATR-FTIR), scanning electron microscopy (SEM), atomic force microscopy (AFM), contact angle measurements, thermogravimetric analysis (TGA), and quantum chemical simulations. While gas permeation investigations were carried out with CO_2/CH_4 mixes to determine separation selectivity and permeability, the pervaporation performance was assessed using a 12/88 wt.% water/isopropanol mixture, which is representative of industrial solvent dehydration scenarios.

2. Materials and Methods

2.1. Materials

Polyetherimide (PEI, Sigma-Aldrich (USA)) was employed as the polymer matrix for membrane fabrication. The Cu-based metal-organic framework HKUST-1 ($Cu_3(BTC)_2$, also known as MOF-199), prepared according to our previous procedure [35], was used as a filler to prepare the MMMs. The synthesized MOF exhibited a specific surface area of 171.6 ± 0.9 m^2 g^{-1} and a particle size of approximately 4 µm [35]. The HKUST-1 structure features three types of cavities: small pores with a size of 0.5 nm, along with two larger pores with diameters of ~1.1 nm and ~1.35 nm, interconnected by channels with a diameter of ~1 nm [37]. N-methyl-2-pyrrolidone (NMP) and isopropanol (iPrOH), procured from Vekton (Russia), were used as received without any further purification [39].

2.2. Membrane Preparation

Dense (nonporous) membranes were fabricated by preparing a 2.5 wt.% PEI solution in NMP, with continuous stirring at 60 °C for 5 hours to ensure complete dissolution of the polymer. The PEI matrix was modified with HKUST-1 at loadings between 0 and 5 wt.% [25]. To ensure a consistent filler dispersion, the resulting PEI and PEI/HKUST-1 dispersions were sonicated at room temperature. Dense membranes were produced by casting these dispersions onto glass Petri dishes and allowing the solvent to evaporate for 24 hours at 60°C in a drying oven. The thickness of the membrane was measured with a micrometer, and the result was approximately 55 ± 10 µm. The membranes' increasing HKUST-1 content was indicated by their labels, which ranged from PEI-0 to PEI-5. Overall, the membrane preparation strategy is in accordance with previously reported techniques for MOF-based MMMs [40].

2.3. Membrane Investigation

2.3.1. Attenuated Total Reflectance Fourier Transform Infrared Spectroscopy (ATR-FTIR)

Using Attenuated Total Reflectance Fourier-transform infrared (ATR-FTIR) spectroscopy, the presence of HKUST-1 and the expected modifications in the membrane matrix were investigated. An IRAffinity-1S instrument (Shimadzu, Kyoto, Japan) fitted with a PIKE Technologies ATR accessory (Moscow, Russia) was used for the measurements. Spectra were collected across the range of 4000 to 450 cm^{-1} at a stable temperature of 25 °C.

2.3.2. Microscopic Methods

The surface and internal structures of the membranes were investigated using SEM with a Zeiss Merlin instrument (Carl Zeiss SMT, Oberkochen, Germany). Cross-sectional imaging was performed by fracturing the membranes in liquid nitrogen, which facilitated the formation of smooth and well-defined fracture surfaces [41]. Surface morphology and topographical characteristics were further analyzed using AFM operated in tapping mode. Measurements were carried out with an NT-MDT NTegra Maximus system (NT-MDT Spectrum Instruments, Moscow, Russia), utilizing silicon cantilevers with a nominal spring constant of 15 N/m.

2.3.3. Contact Angle Measurements

The surface hydrophilic-hydrophobic balance of the developed membranes was analysed using contact angle measurements by the sessile drop method. A goniometer (model LK-1) was used, and the data obtained were processed with DropShape software (developed jointly by Lomonosov Moscow State University and NPK Open Science Ltd., Krasnogorsk, Russia).

2.3.4. Thermogravimetric Analysis (TGA)

A TG 209 F1 Libra thermobalance (Netzsch, Waldkraiburg, Germany) was used to analyse the membranes' thermal stability and breakdown behaviour in an inert argon environment at a heating rate of 10 °C/min.

2.4. Membrane Performance

2.4.1. Pervaporation

The pervaporation performance of the fabricated PEI-based membranes was evaluated using a model azeotropic mixture of isopropanol and water (12 wt.% water) under ambient temperature and steady-state conditions. Cells having an effective membrane area of 9.6 cm^2 were used for the testing, and they were continuously stirred. A Chromatek Crystal 5000.2 gas chromatograph (Chromatec, Nizhny Novgorod, Russia) fitted with a "Hayesep R" column and a thermal conductivity detector was used to determine the compositions of the permeate and feed [42]. Membrane transport performance was evaluated using the following key parameters: permeation flux (J) (Eq.1) and separation factor (β) (Eq. 2) [5]:

$$J = \frac{W}{A \times t} \tag{1}$$

where W is the weight of the permeated components (kg), t is the permeation period (h), and A is the membrane area (m^2) [43];

$$\beta = \frac{y_w / y_{iPrOH}}{x_w / x_{iPrOH}} \tag{2}$$

where x_w and x_{IPA} are feed fractions of components, and y_w and y_{IPA} are permeate fractions of components.

To evaluate membrane performance in comparison, the pervaporation separation index (PSI), expressed in $kg.m^{-2}\cdot h^{-1}$, was calculated using the following Equation 3 [5]:

$$PSI = J \times (\beta - 1) \tag{3}$$

2.4.2. Calculation of Activation Energy

An Arrhenius-type equation, as explained by [44], was used to calculate the activation energy based on transport parameters obtained for membranes:

$$X = X_0 \exp\left(\frac{-Ex}{RT}\right) \tag{4}$$

where X represents the permeation parameter (permeation flux (J)), X_0 is the pre-exponential factor corresponding to J_0, Ex denotes the activation energy for permeation, which varies depending on the specific transport process considered, and R is the gas constant and T, the absolute temperature. To estimate the activation energy, Arrhenius plots of *lnJ* versus *1/T* were constructed, and the results are discussed in the subsequent section.

2.4.3. Gas Permeation

The transport properties in gas separation were assessed using the constant-volume/variable-pressure approach [45]. The membrane had an effective area of 4.9 cm^2 and was mounted in a stainless steel cell [45]. A binary gas mixture of CO_2 and CH_4 (50:50 vol.%) was introduced on the feed side at a pressure of 1 atm, while the permeate side was maintained under vacuum. All measurements were conducted at 25 ± 1 °C. Permeability (P, Barrer) was determined using Equation 5:

$$\mathrm{P} = \frac{273.15Vl}{76AT\Delta \mathrm{p}}\left(\frac{dp}{dt}\right)_{ss} \tag{5}$$

where T is the absolute temperature (K), Δp is the transmembrane pressure difference (atm), $\left(\frac{dp}{dt}\right)_{ss}$ is the steady-state pressure increase rate (torr/s), and V is the downstream volume (cm^3), l is the membrane thickness (cm), and A is the effective membrane area (cm^2) [46].

Ideal selectivity ($\alpha CO_2/CH_4$) was determined as the ratio of single-gas permeabilities measured separately for CO_2 and CH_4. Mixed-gas selectivity was calculated from the ratio of molar fluxes for CO_2 and CH_4 under binary mixture conditions.

After each permeation experiment, the membrane was purged with carrier gas (N_2) at ambient conditions. The time required for complete desorption of CO_2 and CH_4 was monitored using a gas chromatograph connected to the permeate side, providing an assessment of gas retention and sorption kinetics.

2.4.4. Theoretical consideration

Gaussian 16W (Revision A.03) [47]was used to optimize the model molecular structures' geometry, and VMD 1.9.4a [48] was used for visualization. The 6-31G basis set and the PBE0 hybrid functional [49] were used in the optimization and characterization processes. The singlet electronic state was used for all computations. The absence of imaginary vibrational frequencies indicates that the optimized geometries correspond to local minima on the potential energy surface, which was verified using Hessian matrix analysis. Standard conditions (298.15 K, 1 atm) were used to evaluate thermodynamic parameters [50].

For bond order analysis and Bader's Quantum Theory of Atoms in Molecules (QTAIM), the Multiwfn 3.8 software [51] was utilized. Additionally, non-covalent interaction (NCI) plots [52] were generated in VMD, using an isosurface value of 0.5 $(e^{1/3}\,bohr)^{-1}$ and a color scale range of [-0.04; 0.02] e $bohr^{-3}$ to distinguish between attractive, repulsive, and van der Waals interactions [53].

3. Results and Discussion

3.1. Structure of PEI-based Membranes

Structural modifications in the PEI-based membranes upon incorporation of HKUST-1 were analyzed using FTIR spectroscopy, SEM, and AFM. FTIR spectroscopy was performed to investigate potential chemical interactions between the PEI matrix and the MOF filler, as well as to confirm the successful incorporation of HKUST-1 into the polymer structure (Fig. 1).

The pristine PEI membrane displayed characteristic carbonyl symmetrical stretch at 1716 cm^{-1} and asymmetrical stretch at 1774 cm^{-1} for the imide carbonyl group (C=O), 1356, 743 cm^{-1} (C-N), and 1234 cm^{-1} (C-O-C aromatic ether) [54,55]. Upon HKUST-1 incorporation, additional peaks appeared in the region of 1630–1645 cm^{-1} and 1370–1385 cm^{-1}, owing to the stretching bands of the carboxylate groups in the MOF [35]. A weak shoulder around 590-620 cm^{-1} was also observed in the MMMs (PEI-2 and PEI-5), associated with Cu-O stretching vibrations from the paddlewheel structure of HKUST-1. At higher MOF content (for the PEI-5 membrane), peak intensities increased. Furthermore, the introduction of HKUST-1 induced shifts in the C=O vibration bands from 1774 to 1776 cm^{-1} and from 1716 to 1718 cm^{-1}. These shifts can be attributed to intermolecular interactions between the HKUST-1 ligand (BTC) and the imide fragments of PEI (Fig. 1b), which is consistent with the energetically favourable interaction demonstrated in Section 3.3. Concurrently, the positions of the other characteristic PEI peaks remained unchanged. Interestingly, even at a 5 wt.% loading, the positions of the ether group C-O-C vibrations at 1234 cm^{-1} and 1173 cm^{-1} (C-O) remained unchanged. This suggests the presence of steric hindrance that prevents interaction, despite its

energetic feasibility, as discussed in Section 3.3. Thus, the potential for interaction between the imide fragments and the MOF, coupled with the absence of phase separation (as confirmed by the SEM data below), indicates effective dispersion of HKUST-1 within the polymer matrix at low loadings. Conversely, at higher loadings, MOF aggregation and the formation of interfacial defects occur, which is a consequence of the limited number of available imide sites within the PEI structure. The SEM (Fig. 2) and the AFM (Fig. 3) images revealed the morphological alterations induced by HKUST-1 incorporation.

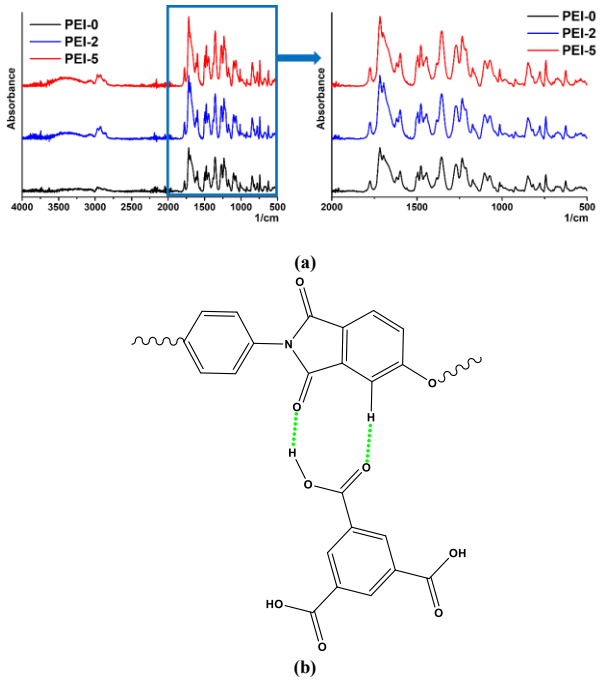


Fig. 1. (a) FTIR spectra of composite membranes before and after filler loadings, (b) a schematic illustration of interactions between the HKUST-1 ligand (BTC) and the imide fragment of PEI.

The SEM micrographs in Fig. 2 display clear morphological changes when different HKUST-1 loadings are added. Similar to those observed in earlier investigations, the pristine PEI membrane (PEI-0) displayed a smooth surface structure and a typical cross-sectional ridge-and-valley morphology [56]. As HKUST-1 was gradually added, the membranes' cross-sections showed more obvious macrovoids. According to this, there can be limited compatibility between HKUST-1 particles and the polymer matrix. This could result in HKUST-1 particle agglomeration and the creation of micro-gaps at the interface, which could affect membrane performance [25]. The PEI-2 membrane, on the other hand, showed a well-balanced structure with uniform void distribution and moderate surface roughness (without "holes"), indicating ideal filler dispersion.

Such macrovoids can function as non-selective transport channels in both pervaporation and gas separation processes, as shown by pervaporation experiments at various temperatures. The membrane morphology changed significantly at higher loadings (PEI-3, PEI-4, PEI-5). As mentioned in the FTIR analysis (Section 3.3), which also controls the changes in transport properties, this is most likely because there are only a few imide sites available for interaction with the MOF. In particular, the surface showed non-hollow "holes" that broke the polymer matrix continuity, producing rough, uneven surfaces with HKUST-1 agglomerates, and the cross-sectional micrographs showed large, spherical, non-selective interfacial voids. While the density of these voids increased when the filler content was increased from 3 to 4 wt.%, the average size of these voids increased threefold for PEI-5, probably due to particle agglomeration. Therefore, the membrane morphology is drastically changed by increasing the HKUST-1 content, producing more textured and heterogeneous surfaces. The PEI-2 membrane stood out with a relatively uniform surface (without «holes» and HKUST-1 agglomeration), suggesting a stable filler distribution. The agglomeration of particles above the optimal concentration in the matrix that concurrently increases roughness can promote non-selective transport and pore blockage, even though increased surface roughness generally improves membrane performance by increasing the effective surface area, creating more accessible sorption sites, and reducing interfacial resistance to facilitate gas uptake and diffusion. Therefore, to achieve improved performance, the ideal MOF loading, which determines the bulk and surface properties of the membrane, must be carefully balanced [57].

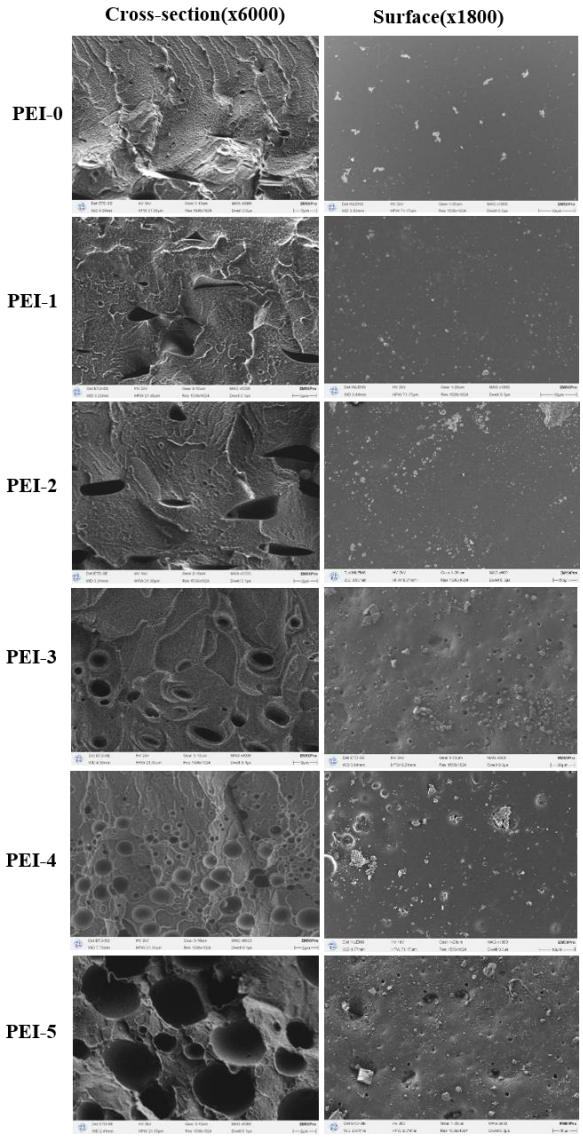


Fig. 2. SEM micrographs of membranes based on PEI and PEI/HKUST-1 composites.

The PEI-based membranes' surface topography and roughness evolution are thoroughly explained by the AFM analysis. The surface AFM images and the corresponding membrane average roughness (Ra) values are shown in Fig. 3.

The surface of the pristine PEI membrane (PEI-0) was relatively smooth and uniform with an Ra of 1.6 nm. Such low surface roughness is in good accordance with the absence of filler. Therefore, the surface of the membrane was flat and homogeneous. With the addition of HKUST-1, it can be clearly seen that the increase in modifier content noticeably raised the surface roughness of MMMs, characterized by the appearance of scattered peaks and valleys. AFM and SEM data are in good agreement, as shown in Fig. 2. Such changes on the surface of PEI-1 and PEI-2 membranes, that is, the increase of effective membrane contact area, may increase membrane-solute interactions and hence contribute to the enhancement of separation performance [58]. In particular, a larger contact area improves the initial sorption of the liquid feed components, which makes the increased effective surface area advantageous for pervaporation applications. However, the formation of "holes," which produce non-selective surface pathways that lower selectivity, and the formation of agglomerates, which hinder transport channels, were the two main causes of the markedly increased surface roughness (observed in PEI-3 to PEI-5) at high modifier loadings (Fig. 2). The moderate roughness of PEI-2 represents the best compromise.

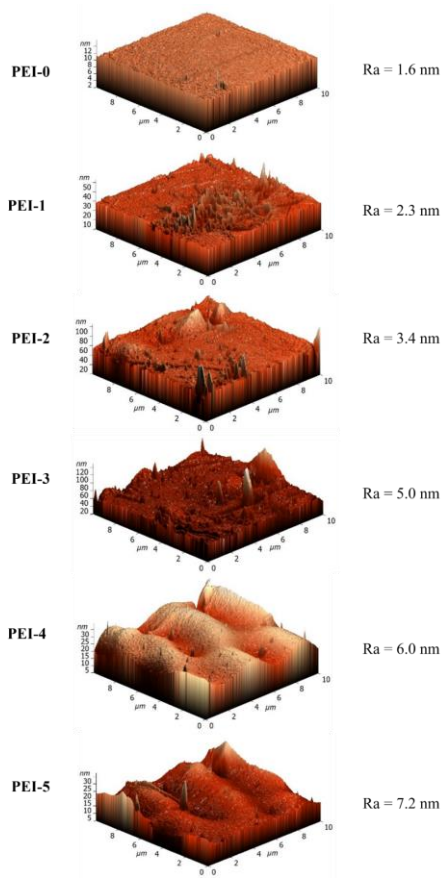


Fig. 3. The surface topography of membranes based on PEI and PEI/HKUST-1 composites.

The PEI-3, PEI-4, and PEI-5 membranes exhibited higher surface roughness values compared to the others, indicating HKUST-1 agglomeration on the membrane surface and phase separation at excessive filler concentrations. These irregular topographies may hinder the component transport through the membrane by forming non-selective defects. Low loadings (1-2 wt.%) of modifier lead to improved polymer-filler compatibility and uniform HKUST-1 dispersion in the polymer matrix, which potentially fills surface irregularities and flattens the topography. Such relatively smooth surfaces may also result from HKUST-1 acting as a nucleating agent during membrane formation [59,60].

3.2. Physicochemical Properties of PEI-based Membranes

The physicochemical properties of the PEI-based membranes were evaluated using water contact angle measurements to determine surface hydrophilicity and by thermogravimetric analysis (TGA). The water contact angle values for PEI and PEI/HKUST-1 composite membranes are presented in Fig. 4.

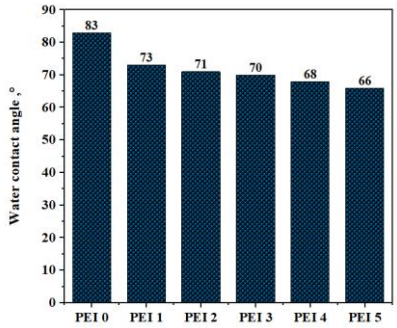


Fig. 4. Water contact angles for membranes based on PEI and PEI/HKUST-1 composites.

The pristine PEI-0 membrane showed a contact angle of 83° (close to previously reported data [61,62]), indicating a relatively hydrophobic surface. With increasing MOF content, the water contact angle progressively decreased, reaching 66° for the PEI-5 membrane. This trend reflects increased surface hydrophilicity, likely arising from the polar functional groups of the HKUST-1 ligand and residual water molecules coordinated within the HKUST-1 structure [63], as it is also confirmed by computational investigation. Moreover, the increase in surface roughness at moderate MOF loadings (the PEI-1 and PEI-2 membranes) may further contribute to enhanced wettability via capillary effects [64]. Improved hydrophilicity can benefit membrane performance by enhancing water flux in aqueous separation processes.

TGA was employed to evaluate the thermal degradation behaviour of neat PEI (PEI-0) and modified with HKUST-1 membranes (PEI-2 and PEI-5). Thermogravimetric curves (TG) for the developed PEI-0, PEI-2, and PEI-5 membranes are presented in Fig. 5.

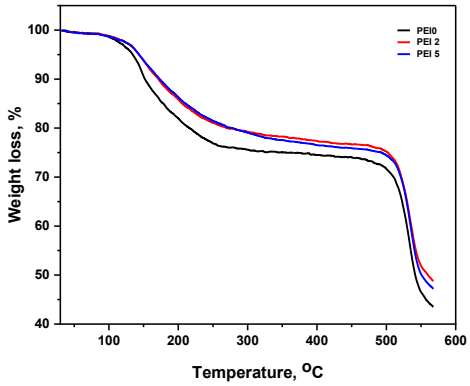


Fig. 5. TG for the developed PEI-0, PEI-2, and PEI-5 membranes.

Although literature typically describes a one-step degradation process for thoroughly dried PEI in the range of 450 to 650°C [29], the PEI-0 sample in this study, as shown in Fig. 5, exhibited a three-step thermal degradation process. Similar behavior has been observed in the work [65]. The first mass loss step, from 30 to 130°C, was associated with the evaporation of adsorbed moisture. The subsequent step was attributed to the removal of residual NMP solvent and to an alteration of the PEI degradation pathway due to the presence of water, as polyimides are hygroscopic polymers [65]. The main thermal decomposition event finally occurred above 550°C. The incorporation of HKUST-1 introduced an additional degradation step between 340 and 490°C, corresponding to the framework decomposition of HKUST-1 [66]. Interestingly, a comparison of the TG curves for the PEI-2 and PEI-5 membranes at temperatures below the decomposition point of HKUST-1 reveals a difference in mass change of approximately 5% compared to the PEI-0 sample, despite the HKUST-1 content being only 2 wt.% relative to the polymer mass for PEI-2. The interactions between the polymer and filler are likely responsible for this enhanced heat stability. The polymer chains' mobility may be limited by these interactions, and the MOF particles themselves serve as thermal insulators, delaying the thermal breakdown process [67,68]. Additionally, the higher residual mass for PEI-2 (48.7%) as opposed to PEI-5 (47.2%) suggests that this MOF loading optimally improves the composite's thermal resistance. On the other hand, excessive loading seems to jeopardize thermal stability and structural integrity, which is consistent with the SEM observations of large interfacial voids and defects in PEI-5. In conclusion, for the developed MMMs, while the introduction of 2 wt.% HKUST-1 enhances thermal stability and indirectly corroborates polymer-filler interaction; the overall thermal stability of the composite remains ultimately limited by the decomposition temperature of HKUST-1 (~340°C).

3.3. Quantum-Chemical Studies for PEI-based Membranes

Transport phenomena and physicochemical properties in composite systems can be predicted and explained using quantum-chemical studies, which are an effective research tool. These investigations help optimize membrane structures for improved performance and clarify current structure-property relationships by offering insights into molecular-level interactions between MOF modifiers and polymers [42]. The study of noncovalent interactions between MOFs and polymers is given special attention in this context. Composite membrane behavior is greatly influenced by hydrogen bonding and other noncovalent interactions, such as ionic interactions and van der Waals

forces. By comprehending these mechanisms, researchers can modify these materials for increased durability and separation efficiency [27].

In this study, the model systems utilized included molecules of H_2O, iPrOH, benzene-1,3,5-tricarboxylic acid (BTC, HKUST-1 ligand), as well as hydrophilic (PEI-I) and hydrophobic (PEI-II) fragments of PEI (Fig. 6). These segments were used to investigate the hypothetical interactions between components of the feed mixture and different regions of PEI with varying hydrophilicity. Based on the geometries of the optimized structures, hypothetical molecular associates were generated and further optimized to characterize their interactions. Multiple interaction scenarios were considered for each pair. However, post-processing was conducted only for the most energetically favorable associates. Table S1 in the Supplementary Information lists the XYZ coordinates of both the initial molecules and their formed associates.

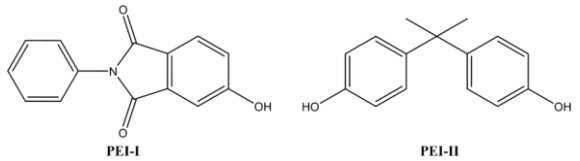


Fig. 6. Model PEI-I and PEI-II systems.

The change in thermodynamic potentials during association was obtained as the difference between the energy of the complex and the initial model molecules. Accordingly, Table S2 of the Supplementary Information presents the change in Gibbs free energy and enthalpy obtained under standard conditions. Table 1 provides the change in isothermal-isobaric potentials for the most energetically favorable associates.

Table 1
Standard Gibbs free energy changes during the formation of the most energetically favourable associates.

ΔG_{min}, kJ/mol			
PBE0/6-31G	**BTC**	**H_2O**	**iPrOH**
PEI-I	-17.1	4.4	9.7
PEI-II	23.6	13.5	19.9
PEI-II(OH)	-12.2	3.9	8.6
BTC	~	-37.0	-32.6
H_2O		~	-2.6

Based on the obtained values of the Gibbs free energy change, the poor affinity of the mixture components (H_2O, iPrOH) for the PEI material was demonstrated. The higher water contact angle observed for the PEI membrane is in agreement with the above observation (Fig. 4). However, when considering the energy change in the case of interactions between water and iPrOH with the HKUST-1 ligand, a significant energy gain was observed (-37.0 and -32.6 kJ/mol, respectively), which would lead to greater swelling of the membranes in the separated mixture and facilitated transport upon MOF incorporation. Additionally, when examining the interactions between BTC and PEI, it was noted that hydrophilic BTC poorly interacts with the hydrophobic fragment of PEI-II. At the same time, effective interaction was observed between BTC and the imide segment (PEI-I), as well as efficient interaction with the hydroxy group of the PEI-II(OH) fragment, which corresponds to the obtained uniform distribution of HKUST-1 within the polymer matrix (Fig. 2). The interaction with the imide group was further confirmed by the characteristic peak shifts in the FTIR spectrum of the composite (Fig. 1). In contrast, no such shifts were detected for the ether group. This absence of a signal could be attributed to the limitations of the computational model, which utilized a hydroxy group as a simpler analogue for the ether moiety, as well as potential steric hindrances that limit access to the oxygen lone pair in the actual ether group, factors not accounted for in the present study.

The non-covalent nature of the interactions during the formation of associates was confirmed through topological analysis and measurement of bond lengths and orders using Multiwfn 3.8 software. QTAIM analysis revealed the presence of bond critical points and bond paths [41]. The noncovalent interactions were analyzed using the obtained NCI plots (Fig. 7 and Fig. S1 in the Supplementary Information), where hydrogen bonds are indicated in blue, van der Waals interactions in green, and steric repulsion in red.

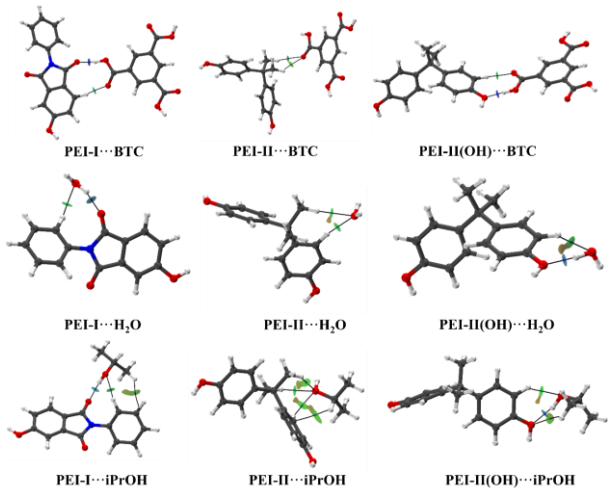


Fig. 7. The NCI plot index isosurfaces and QTAIM distribution of BCPs (blue spheres), as well as bond paths for the associates with PEI-I and PEI-II.

The strength of the interactions was assessed based on the calculated Wiberg Bond Indexes (WBI) [69,70] and the Fuzzy bond orders (FBO) [71]. Table 2 presents the bond orders and the ratio (R) of the distance between interacting atoms (L) to the sum of their van der Waals radii [72]. Additionally, an evaluation of the hydrogen interaction energy was conducted based on real-space function values at bond critical points, as described in work [73]. The results are presented in Table S3 of the Supplementary Information.

Table 2
Values of Wiberg Bond Index and Fuzzy Bond Order, distance between interacting atoms (L), and the ratio of it to the total of van der Waals radii (R).

PBE0/6-31G						
Associate		**Interaction**	**WBI**	**FBO**	**L, Å**	**R, %**
PEI-I	BTC	H///O(CO*OH)	0.043	0.056	2.1055	77.4%
		O///H(COOH)	0.130	0.103	1.6483	60.6%
	H_2O	H///O	0.035	0.044	2.3198	85.3%
		O///H	0.071	0.064	1.8554	68.2%
	iPrOH	O///H(OH)	0.071	0.063	1.8569	68.3%
		H///O	0.033	0.043	2.2576	83.0%
PEI-II	BTC	H(CH3)///O(CO*OH)	0.008	0.022	2.7525	101.2%
		H(CH3)*///O(CO*OH)	0.007	0.021	2.7268	100.2%
	H_2O	H(CH3)///O	0.018	0.033	2.5598	94.1%
		H(CH)///O	0.027	0.044	2.2851	84.0%
	iPrOH	H(CH3)///O	0.010	0.021	2.7948	102.7%
		H(CH3)*///O	0.016	0.034	2.4821	91.3%
		H(CH)///O	0.009	0.023	2.5855	95.1%
PEI-II (OH)	BTC	O///H(COOH)	0.134	0.115	1.6352	60.1%
		H(CH)///O(CO*OH)	0.028	0.042	2.2925	84.3%
	H_2O	O///H	0.083	0.075	1.8302	67.3%
		H(CH)///O	0.028	0.040	2.3772	87.4%
	iPrOH	O///H(OH)	0.080	0.071	1.8514	68.1%
		H(CH)///O	0.024	0.035	2.4217	89.0%
		O///H(CH3)	0.004	0.015	2.9721	109.3%
BTC	H_2O	O(CO*OH)///H	0.076	0.062	1.9308	71.0%
		H(COOH)///O	0.161	0.143	1.5724	57.8%
	iPrOH	O(CO*OH)///H	0.066	0.054	1.9989	73.5%
		H(COOH)///O	0.162	0.135	1.5691	57.7%
H_2O	iPrOH	O///H(OH)	0.107	0.100	1.7693	65.0%

Based on the NCI plots (Fig. 7), the primary types of interactions are hydrogen bonding and van der Waals forces. In the case of PEI, these interactions are attributed to oxygen-containing hydroxy and imine groups. The system discussed in this work appears to exhibit optimal modifier content. At low HKUST-1 loadings (≤2 wt.%), interactions between the BTC linker and the PEI matrix may induce cross-linking of the polymer chains, which helps to maintain high selectivity [5]. However, a further increase in filler content (>2 wt.%) leads to a significant change in morphology, characterized by the

formation and growth of interfacial voids in terms of both quantity and size, as observed in the cross-section SEM images (Fig. 2). This phenomenon is likely due to the limited number of oxygen-containing sites in PEI available for strong intermolecular interactions with the modifier. Saturation of these sites encourages the development of interfacial defects. The diffusion of hydrophilic components through the membrane is additionally hindered by matrix densification caused by BTC-PEI interactions and the HKUST-1's blocking of the polymer's functional groups. As observed in Section 3.4.1 (Fig. 8), this causes a decrease in permeation flux while maintaining high separation selectivity upon an increase in HKUST-1 content [31].

Analysis of the R values and bond orders (Table 2) reveals that the obtained WBI values < 0.3 indicate the formation of non-covalent interactions [74]. Additionally, the calculated WBI values are consistent with the Gibbs free energy changes (Table 1) and the estimated hydrogen bond energies (Table S3 in Supplementary Information). Notably, the WBI values for hydrogen bonds between water and BTC are higher than those for the PEI···H_2O system (0.161 > 0.083 > 0.071 for BTC, PEI-II(OH), and PEI-I, respectively), which correlates with the observed hydrophilization of the composite membrane surfaces (Fig. 4) and the improved permeation flux due to enhanced sorption of feed components on the membrane surface.

3.4. Transport characteristics of PEI-based Membranes

3.4.1. Pervaporation Performance

The pervaporation performance of PEI-based MMMs with varying HKUST-1 loadings was assessed using an azeotropic water/isopropanol mixture (12 wt.% water), as shown in Fig. 8.

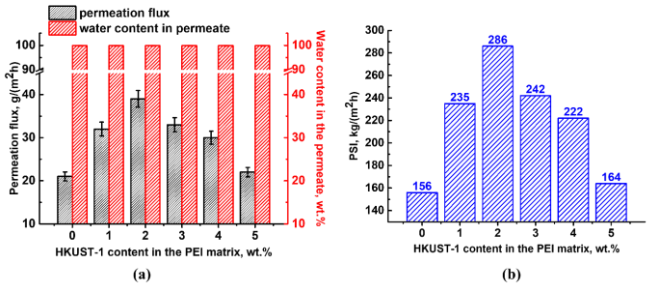


Fig. 8. Transport parameters **(a)** permeation flux and water content in the permeate, **(b)** PSI of the developed PEI-based membranes in pervaporation dehydration of iPrOH (12 wt.% water).

The effect of HKUST-1 loading in the PEI matrix on pervaporation performance was evaluated based on permeation flux and water content in the permeate. The water content in the permeate for all membranes remained consistently high at 99.9 wt.%, indicating that the membranes maintained excellent selectivity for water regardless of the MOF loading. This consistent high purity indicates that incorporating HKUST-1 preserves selective water permeation, which aligns with a molecular sieving mechanism, as isopropanol molecules (1.6 nm) are too large to penetrate the HKUST-1 pores (0.5, 1.1, and 1.35 nm).

The permeation flux values indicate a general trend of increasing membrane permeation flux with the addition of MOF. This behaviour can be interpreted through the solution-diffusion model, which is the primary mechanism for separation in dense membranes. Therefore, a number of factors are responsible for the observed increase in permeation flux when compared to the unmodified PEI-0 membrane. These include an enhanced hydrophilicity of the modified membrane surface (confirmed by contact angle data, Fig. 4), which encourages the preferential sorption of polar water molecules, and an increased sorption contribution due to increased surface roughness (confirmed by AFM, Fig. 3). This is combined with the addition of porous and hydrophilic HKUST-1, which serves as extra water pathways [75] and, according to computational techniques, promotes diffusion because of favorable interactions with feed components. Finally, the optimization of the modifier content was crucial, as it promoted a uniform dispersion of the HKUST-1 filler within the polymer matrix and a defect-free morphology. When MOF was added to the PEI matrix up to 2 wt.%, the permeation flux increased and reached a maximum of about 39 $g.m^{-2}.h^{-1}$, all the while maintaining high selectivity with a water content of about 99.9 wt.% in the permeate. A decline in permeation flux was observed at loadings exceeding 2 wt.%, due to morphological changes, specifically, the formation of micro-gaps at the interface caused by a reduced number of accessible hydrophilic groups on the PEI (confirmed earlier by computational methods) and MOF agglomeration (confirmed by SEM, Fig. 2). These factors collectively hinder effective component transport [53].

When the HKUST content is increased to 2 wt.% loading, the PSI values clearly show an improvement, peaking at 286. This increase is a result of the synergistic effects of PEI and HKUST-1, which improve permeability and selectivity. The PSI values started to decrease as the MOF loading increased above this threshold, which is consistent with the permeation flux decrease that was noted. This decrease could be an indication that high filler loading reduces the interfacial contact between PEI and HKUST-1 and may cause filler agglomeration, which would be negative to the membrane's overall performance [25]. The most balanced composition in terms of both structural stability and performance is HKUST-1.

The effect of operating temperature on the pervaporation performance of the optimal PEI-2 membranes was also evaluated (Fig. 9). The data for the PEI-0 are presented for comparison. For both membranes, the permeation flux values indicate a distinct trend of increasing with temperature. This is explained by the higher mobility of water molecules at higher temperatures, as well as the extra pathways that the MOF for the PEI-2 membrane provides, which enable more effective transport through the membrane. At 22 °C, the permeate's water content was maintained high in each of the samples. But for the PEI-0 and PEI-2 membranes, this decreased at 35 and 50°C, suggesting that higher temperatures could result in increased permeation of other components and decreased selectivity.

The formation of non-selective interfacial voids (confirmed by SEM), which leads to increased polymer chain mobility at high temperatures, could be the cause of the modified PEI-2 membrane's lower water concentration in the permeate as compared to the PEI-0 membrane. The water selectivity of the modified membrane may be compromised by these defects, which could also act as preferred pathways for the co-permeation of organic components [2,33].

For both types of membranes, PSI values decrease with temperature, indicating that while higher temperatures increase permeation flux, they also adversely affect membrane selectivity to the point where overall separation efficiency is decreased. The PEI-2 membrane, however, shows greater PSI values, indicating its potential.

The Arrhenius relationship (Eq. 4) was used to calculate the corresponding activation energies (Ea) based on the data of iPrOH pervaporation dehydration at high temperatures (22-50 °C). The Arrhenius plot's slope (lnJ vs. 1/T) was used to calculate the Ea for water transport through the membranes (Fig. 10).

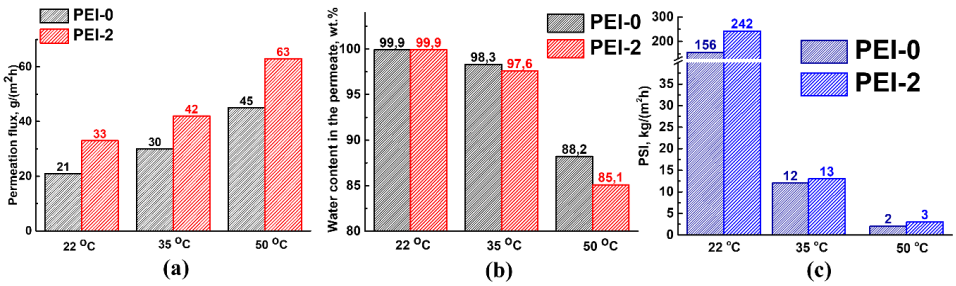


Fig. 9. Transport parameters (**(a)** permeation flux, **(b)** water content in the permeate, **(c)** PSI) of the developed PEI-based membranes in pervaporation dehydration of iPrOH (12 wt.% water) at elevated temperatures (22-50 °C).

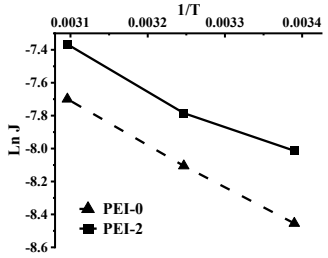


Fig. 10. Variation in lnJ with temperature for the PEI-0 and PEI-2 membranes in pervaporation dehydration of IPA (12 wt.% water).

The PEI-2 membrane showed a lower Ea of 18.3 kJ/mol, while the pristine PEI-0 membrane displayed an Ea of 21.4 kJ/mol. The addition of HKUST-1 facilitated water transport, as evidenced by the lower activation energy for PEI-2, indicating that water molecules require less energy to pass through the membrane. These results indicate that a moderate HKUST-1 loading (2 wt.%) in the PEI matrix decreases the energy barrier for mass transport while simultaneously improving membrane permeability. The outcomes are in accordance with earlier research showing that MOF can produce more channels in polymer matrices, enhancing membrane performance overall [20].

3.4.2. Gas Separation Performance

The gas separation performance of the PEI-0 and PEI-2 membranes was evaluated using a biogas mixture of CO_2 and CH_4. The key parameters analysed were gas permeability (P, Barrer) and selectivity (Table 3).

The CO_2 and CH_4 permeabilities of the pristine PEI-0 membrane were 12.1 and 3.48 Barrer, respectively. The mixed-gas selectivity was slightly lower at 3.46, whereas the optimal selectivity for CO_2/CH_4 was determined as 3.52. However, after carrier gas purging, gas desorption from the membrane was significantly slow, with CO_2 residues remaining for up to 4 hours and CH_4 residues for about 1.5 hours. Strong sorption interactions between the PEI matrix and the gas molecules, especially CO_2, are indicated by this prolonged retention, which is consistent with PEI's known affinity for polarizable gases [76].

The permeability greatly increased with the addition of 2 wt.% HKUST-1 (the PEI-2 membrane). The CO_2 and CH_4 permeabilities of the modified membrane were 38.1 and 35.7 Barrer, respectively. However, there was a significant decline in separation performance as the CO_2/CH_4 selectivity dropped to 1.07 (mixed gas) and 0.76 (ideal conditions). This significant decrease in selectivity points to the existence of non-selective flaws in the membrane structure, which may be caused by the polymer-MOF interfacial compatibility (verified by SEM and computational techniques) [77]. This behavior indicates that gases were able to avoid the MOF's intrinsic porosity because the interfacial region between the PEI matrix and the HKUST-1 crystals did not form a fully continuous, sealed interface. Therefore, the limited number of available imide sites for interaction appears to compromise the homogeneity of the PEI matrix, even though computational modeling has shown that the BTC linker can interact with the imide fragment effectively, as confirmed by FTIR peak shifts. A "sieve-in-a-cage" morphology is created as a result, allowing for indiscriminate gas flow [78]. The molecular sieving contribution of the HKUST-1 pores is overshadowed by these interfacial voids, which function as rapid, low-resistance channels for both gases. Consequently, the intrinsic pore structure of HKUST-1 becomes bypassed by these fast, non-selective leakage pathways. This explains the observed increase in gas permeability for both components without a corresponding improvement in selectivity.

Furthermore, PEI-2 still exhibited slow gas desorption, demonstrating that while diffusion resistance decreased (reflected in higher permeability), sorption interactions with both the polymer and MOF domains remained significant. This combination of strong sorption (retention) and defect-assisted diffusion (fast permeation) results in a mixed transport regime where the separation performance becomes dominated by structural imperfections rather than intrinsic material properties. Thus, the overall transport behaviour results from a combined effect of (i) enhanced free-volume and disrupted polymer packing, (ii) interfacial gaps overriding molecular sieving, and (iii) persistent sorption-controlled kinetics. Therefore, the unexpectedly low selectivity of the PEI-2 membrane is attributed to interfacial micro-defects rather than the intrinsic behaviour of HKUST-1. Future efforts should focus on improving polymer–MOF interfacial compatibility through HKUST-1 surface functionalization or PEI end-group modification to suppress non-selective defects and better harness the intrinsic sieving capability of HKUST-1.

3.5. Performance Comparison of PEI-based Membranes

The transport properties of the developed PEI/HKUST-1 (2%) membrane (PEI-2) were compared to those of commercial PEI-based analogues (Ultem 1000™ and Ultem 1010™) (Table 4). To the best of our knowledge, this study represents one of the first works exploring PEI-based membranes for pervaporation applications in isopropanol dehydration, addressing a significant gap in the existing literature. The developed membrane was shown to have improved permeation flux and/or water selectivity compared to commercial membranes.

The gas separation performance of the PEI-2 membrane was also compared to that of the PEI-based membranes described in the literature for a biogas mixture of CO_2 and CH_4 under conditions close to this study (Table 5). Based on these data, it was noted that the developed membrane was shown to have improved gas CO_2 permeability in biogas, but was inferior in selectivity. However, it is worth noting that it is quite difficult to compare the data presented in the literature due to the different experimental conditions and the expression of the obtained performance parameters in different units of measurement.

Table 3
Gas permeability and selectivity of the PEI-0 and PEI-2 membranes.

Membrane	Permeability (P), Barrer				Selectivity	
	CO_2 (in biogas)	CH_4 (in biogas)	CO_2	CH_4	CO_2/CH_4 (in biogas)	CO_2/CH_4 (ideal)
PEI-0	12.1	3.48	11.8	3.36	3.46	3.52
PEI-2	38.1	35.7	34.8	45.8	1.07	0.76

Table 4
Pervaporation performance of PEI-based membranes in isopropanol dehydration.

Membrane	Tem-re, °C	Water content in the feed, wt.%	Permeation flux, $g \cdot m^{-2} \cdot h^{-1}$	Water content in permeate, wt.%	Reference
PEI/HKUST-1 (2%)	22	12	39	99.9	This study
PEI/HKUST-1 (2%)	50	12	63	85.1	This study
Ultem 1000™	25	12	32	74	[79]
Ultem 1010™	60	15	7	99	[80]

Table 5
Gas separation performance of PEI-based membranes.

Membrane	P_{CO2} (in biogas), Barrer	Selectivity CO_2/CH_4 (in biogas)	Selectivity CO_2/CH_4 (ideal)	Reference
PEI/HKUST-1 (2%)	38.1	1.07	0.76	This study
PEI/graphene (0.1%)	9.93	5.83	-	[81]
PEI/acid-treated graphene (0.1%)	8.93	5.16	-	[81]
PEI/polyvinyl acetate (4%)	-	-	26.15	[82]
PEI/polyimide	-	16.6	-	[83]

4. Conclusions

Novel MMMs based on PEI modified with HKUST-1 were developed and investigated for dual functionality in pervaporation and gas separation applications. The influence of HKUST-1 loading on the pervaporation performance of PEI-based MMMs was systematically investigated using an azeotropic isopropanol/water mixture (12 wt.% water). The HKUST-1 content in the membranes varied from 1 to 5 wt.%, and the results revealed that increasing the MOF content initially enhanced the permeation flux while maintaining high selectivity, with the water content in the permeate reaching 99.9 wt.%.This improvement was attributed to several factors, including morphological changes observed by SEM, increased surface roughness confirmed by AFM, enhanced surface hydrophilicity as can be seen by contact angle measurements, and the addition of HKUST-1, which provided more water transport pathways and facilitated advantageous interactions with feed components, as confirmed by computational analysis. However, morphological changes, such as micro-gap formation at the interface due to a decrease in accessible hydrophilic groups on the PEI (confirmed by computational methods) and MOF agglomeration (confirmed by SEM), which together hinder component transport, were found to be responsible for the decline in permeation flux at HKUST-1 loadings above 2 wt.%. with the highest permeation flux (~39 $g \cdot m^{-2} \cdot h^{-1}$) and a pervaporation separation index (PSI) of 286, the PEI-2 sample (containing 2wt.% HKUST-1) demonstrated the best separation performance among all the tested membranes.

Further analysis of PEI-2 was done between 22 and 50 °C. Compared to the unmodified PEI membrane, the computed activation energy for water transport through this membrane was 18.3 kJ/mol. This decreased value indicated that the addition of HKUST-1 improved water diffusion by reducing the energy barrier for permeation, as confirmed by FTIR analysis. TGA was also used to confirm the polymer-filler interaction for the PEI-2 membrane.

This membrane's ability to separate gases was evaluated as well using a CO_2 and CH_4 biogas mixture. In comparison to the pristine PEI membrane, the PEI-2 membrane showed a significant increase in permeability for CO_2 and CH_4 (38.1 and 35.7 Barrer, respectively). However, selectivity decreased as a result of this improvement (CO_2/CH_4 = 1.07), suggesting that non-selective defects or pathways partially controlled transport. These defects overshadow the intrinsic porosity of HKUST-1 by creating bypass channels because of poor polymer-MOF compatibility. These defects in structure cause faster, non-specific gas flow, which increases permeability but degrades separation performance even though the MOF is still able to interact with gases. Enhancing polymer–MOF interfacial adhesion is crucial for successful membrane development, according to the results. Combining a physical blending approach with a thermally robust PEI matrix and moderate MOF loading presents a promising strategy for creating multifunctional membranes for industrial separation applications.

Acknowledgments

The authors acknowledge the use of equipment and facilities provided by the Resource Centers for Nanotechnology, Cryogenic Department, Thermogravimetric and Calorimetric Research Centre, Computing Centre, Chemical Analysis and Materials Research Centre, and the Centre of Nanofabrication of Photoactive Materials (Nanophotonics) at St. Petersburg State University.

CRediT authorship contribution statement

G. Thankachan: Investigation, Writing - original draft, Writing - review & editing.
M. Dmitrenko: Formal analysis, Investigation, Writing - original draft, Writing - review & editing, Visualization.
A. Kuzminova: Conceptualization, Investigation, Data curation.
R. Dubovenko: Formal analysis, Investigation, Writing - original draft, Visualization.
U. K. Aravind: Methodology, Supervision, Funding acquisition.
C. T. Aravindakumar: Methodology.
M. Shalygin: Methodology.
L. Gasanova: Investigation.
A. Penkova: Conceptualization, Methodology, Supervision, Project administration, Writing -review & editing, Funding acquisition.

Funding Declaration

This work was supported by the Scheme for Promotion of Academic and Research Collaboration (SPARC) under Grant No. P2411; and Saint Petersburg State University under Grant No. 102591880.

Consent to participate

The authors consented to participate in this study.

Data availability

Availability of data and materials will be made available upon reasonable request.

Declaration of Interest Statement

The authors report there are no competing interests to declare.

References

[1] S.R. Kafle, S. Adhikari, R. Shrestha, S. Ban, G. Khatiwada, P. Gaire, N. Tuladhar, G. Jiang, A. Tiwari, Advancement of membrane separation technology for organic pollutant removal, Water Science and Technology 89 (2024) 2290–2310. https://doi.org/10.2166/wst.2024.117.

[2] X. Xu, Y. Hartanto, J. Zheng, P. Luis, Recent Advances in Continuous MOF Membranes for Gas Separation and Pervaporation, Membranes 12 (2022). https://doi.org/10.3390/membranes12121205.

[3] S. Zid, P. Alcouffe, M. Zinet, E. Espuche, Mixed-Matrix Membranes Based on Polyetherimide, Metal–Organic Framework and Ionic Liquid: Influence of the Composition and Morphology on Gas Transport Properties, Polymers 14 (2022) 3489. https://doi.org/10.3390/polym14173489.

[4] A. Kuzminova, M. Dmitrenko, A. Mazur, S. Ermakov, A. Penkova, Novel Pervaporation Membranes Based on Biopolymer Sodium Alginate Modified by FeBTC for Isopropanol Dehydration, Sustainability 13 (2021) 6092. https://doi.org/10.3390/su13116092.

[5] M. Dmitrenko, O. Mikhailovskaya, R. Dubovenko, A. Kuzminova, D. Myznikov, A. Mazur, K. Semenov, Y. Rusalev, A. Soldatov, S. Ermakov, A. Penkova, Pervaporation Membranes Based on Polyelectrolyte Complex of Sodium Alginate/Polyethyleneimine Modified with Graphene Oxide for Ethanol Dehydration, Polymers 16 (2024) 1206. https://doi.org/10.3390/polym16091206.

[6] V. Polyakov, M. Dmitrenko, M. Kalmakhelidze, A. Kuzminova, R. Dubovenko, E. Mukhanova, A. Soldatov, A. Penkova, Development and Characterization of PVA Membranes Modified with In(BTC) Metal–Organic Framework for Sustainable Pervaporation Separation of Isopropanol/Water, Sustainability 16 (2024) 10257. https://doi.org/10.3390/su162310257.

[7] Y.M. Xu, T.S. Chung, High-performance UiO-66/polyimide mixed matrix membranes for ethanol, isopropanol and n-butanol dehydration via pervaporation, Journal of Membrane Science 531 (2017) 16–26. https://doi.org/10.1016/j.memsci.2017.02.041.

[8] Y. Li, B. Huo, Z. Xu, H. Qi, X. Li, P. Cui, Z. Zhu, Y. Wang, J. Yang, J. Gao, Energy-saving and environmentally friendly pervaporation-distillation hybrid process for alcohol and ester recovery from wastewater containing three binary azeotropes, Separation and Purification Technology 281 (2022) 119889. https://doi.org/10.1016/j.seppur.2021.119889.

[9] A. Khazaei, V. Mohebbi, R.M. Behbahani, S.A. Ahmad Ramazani, Energy consumption in pervaporation, conventional and hybrid processes to separate toluene and i-octane, Chemical Engineering and Processing - Process Intensification 128 (2018) 46–52. https://doi.org/10.1016/j.cep.2018.04.009.

[10] N.F. Himma, A.K. Wardani, N. Prasetya, P.T.P. Aryanti, I.G. Wenten, Recent progress and challenges in membrane-based O 2 /N 2 separation, Reviews in Chemical Engineering 35 (2019) 591–625. https://doi.org/10.1515/revce-2017-0094.

[11] X. Liu, J. Wang, L. Fang, Y. Ban, A. Li, M. He, Fabrication of MOFs/PDMS mixed matrix membranes and defect-free composite membranes for efficient air separation, Journal of Nanoparticle Research 26 (2024) 174. https://doi.org/10.1007/s11051-024-06061-9.

[12] R. Castro-Muñoz, M. Zamidi Ahmad, M. Malankowska, J. Coronas, A new relevant membrane application: CO2 direct air capture (DAC), Chemical Engineering Journal 446 (2022) 137047. https://doi.org/10.1016/j.cej.2022.137047.

[13] M. Zunita, R. Hastuti, A. Alamsyah, K. Khoiruddin, I.G. Wenten, Ionic Liquid Membrane for Carbon Capture and Separation, Separation & Purification Reviews 51 (2022) 261–280. https://doi.org/10.1080/15422119.2021.1920428.

[14] S. Rao, B. Prasad, Y. Han, W.S.W. Ho, Polymeric Membranes for H2S and CO2 Removal from Natural Gas for Hydrogen Production: A Review, Energies 16 (2023) 5713. https://doi.org/10.3390/en16155713.

[15] I.U. Khan, M.H.D. Othman, A. Jilani, A.F. Ismail, H. Hashim, J. Jaafar, A.K. Zulhairun, M.A. Rahman, G.U. Rehman, ZIF-8 based polysulfone hollow fiber membranes for natural gas purification, Polymer Testing 84 (2020) 106415. https://doi.org/10.1016/j.polymertesting.2020.106415.

[16] F. Feng, J. Wu, M. Weber, S. Zhang, T.-S. Chung, Facile infiltration of polyethyleneimine as a strong CO2 retardant in scalable dual-polymer membranes for H2/CO2 separation, Journal of Membrane Science 711 (2024) 123217. https://doi.org/10.1016/j.memsci.2024.123217.

[17] A. Li, J. Chu, S. Huang, Y. Liu, M. He, X. Liu, Machine learning-assisted development of gas separation membranes: A review, Carbon Capture Science & Technology 14 (2025) 100374. https://doi.org/10.1016/j.ccst.2025.100374.

[18] X. Xu, D. Nikolaeva, Y. Hartanto, P. Luis, MOF-based membranes for pervaporation, Separation and Purification Technology 278 (2022) 119233. https://doi.org/10.1016/j.seppur.2021.119233.

[19] P. Gkotsis, P. Kougias, M. Mitrakas, A. Zouboulis, Biogas upgrading technologies – Recent advances in membrane-based processes, International Journal of Hydrogen Energy 48 (2023) 3965–3993. https://doi.org/10.1016/j.ijhydene.2022.10.228.

[20] G. Liu, W. Jin, Pervaporation membrane materials: Recent trends and perspectives, Journal of Membrane Science 636 (2021) 119557. https://doi.org/10.1016/j.memsci.2021.119557.

[21] R. Sidhikku Kandath Valappil, N. Ghasem, M. Al-Marzouqi, Current and future trends in polymer membrane-based gas separation technology: A comprehensive review, Journal of Industrial and Engineering Chemistry 98 (2021) 103–129. https://doi.org/10.1016/j.jiec.2021.03.030.

[22] A.A. Shamsabadi, A. Kargari, M.B. Babaheidari, S. Laki, H. Ajami, Role of critical concentration of PEI in NMP solutions on gas permeation characteristics of PEI gas separation membranes, Journal of Industrial and Engineering Chemistry 19 (2013) 677–685. https://doi.org/10.1016/j.jiec.2012.10.006.

[23] A. Pulyalina, V. Rostovtseva, I. Faykov, N. Saprykina, A. Golikova, A. Fedorova, G. Polotskaya, A. Novikov, Impact of Layered Perovskite Oxide La0.85Yb0.15AlO3 on Structure and Transport Properties of Polyetherimide, International Journal of Molecular Sciences 24 (2022) 715. https://doi.org/10.3390/ijms24010715.

[24] A. Bourassi, E.H. Martin, M. Bourre, V. Fila, J. Gaalova, Separation of Diethyl Phthalate From Water by Pervaporation, WSEAS TRANSACTIONS ON ENVIRONMENT AND DEVELOPMENT 17 (2021) 81–87. https://doi.org/10.37394/232015.2021.17.9.

[25] Y. Wang, G. Yang, H. Guo, X. Meng, G. Kong, Z. Kang, R. Guillet-Nicolas, S. Mintova, Preparation of HKUST-1/PEI mixed-matrix membranes: Adsorption-diffusion coupling control of small gas molecules, Journal of Membrane Science 643 (2022) 120070. https://doi.org/10.1016/j.memsci.2021.120070.

[26] R.M.M. Ferreira, A. Ambrosi, T.F. da Conceição, Post-polymerization modification of polyetherimide by Friedel-Crafts acylation: Physical–chemical characterization and performance as gas separation membrane, Journal of Applied Polymer Science 139 (2022) 1–11. https://doi.org/10.1002/app.52330.

[27] Y. Duan, L. Li, Z. Shen, J. Cheng, K. He, Engineering Metal-Organic-Framework (MOF)-Based Membranes for Gas and Liquid Separation, Membranes 13 (2023) 480. https://doi.org/10.3390/membranes13050480.

[28] S. Gunes-Durak, Development of microfiltration membranes based on polysulfone and polyetherimide blends, Water Science and Technology 89 (2024) 2558–2576. https://doi.org/10.2166/wst.2024.135.

[29] S. Zid, P. Alcouffe, M. Zinet, E. Espuche, Mixed-Matrix Membranes Based on Polyetherimide, Metal–Organic Framework and Ionic Liquid: Influence of the Composition and Morphology on Gas Transport Properties, Polymers 14 (2022). https://doi.org/10.3390/polym14173489.

[30] S. Manshad, M.R. Sazegar, Mohd.G. Mohd. Nawawi, H. bin Hassan, Fabrication of nanohybrid polyetherimide/graphene oxide membranes: biofuel dehydration by pervaporation process, RSC Advances 6 (2016) 103888–103894. https://doi.org/10.1039/C6RA22104A.

[31] H. Furukawa, K.E. Cordova, M. O'Keeffe, O.M. Yaghi, The Chemistry and Applications of Metal-Organic Frameworks, Science 341 (2013) 1230444. https://doi.org/10.1126/science.1230444.

[32] R. Dubovenko, A. Kuzminova, M. Dmitrenko, A. Stepanova, A. Selyutin, R. Su, A. Penkova, Enhanced Sodium Alginate Membranes Modified with Metal–Organic Frameworks Based on Zirconium for Energy-Efficient Isopropanol Dehydration by Pervaporation, ACS Applied Polymer Materials 6 (2024) 12675–12690. https://doi.org/10.1021/acsapm.4c02229.

[33] S. Sorribas, A. Kudasheva, E. Almendro, B. Zornoza, Ó. de la Iglesia, C. Téllez, J. Coronas, Pervaporation and membrane reactor performance of polyimide based mixed matrix membranes containing MOF HKUST-1, Chemical Engineering Science 124 (2015) 37–44. https://doi.org/10.1016/j.ces.2014.07.046.

[34] C.Y. Chuah, W. Li, S.A.S.C. Samarasinghe, G.S.M.D.P. Sethunga, T.-H. Bae, Enhancing the CO2 separation performance of polymer membranes via the incorporation of amine-functionalized HKUST-1 nanocrystals, Microporous and Mesoporous Materials 290 (2019) 109680. https://doi.org/10.1016/j.micromeso.2019.109680.

[35] R. Dubovenko, M. Dmitrenko, A. Mikulan, M. Puzikova, I. Dzhakashov, N. Rakovskaya, A. Kuzminova, O. Mikhailovskaya, R. Su, A. Penkova, Thin-Film Composite Polyamide Membranes Modified with HKUST-1 for Water Treatment: Characterization and Nanofiltration Performance, Polymers 17 (2025) 1137. https://doi.org/10.3390/polym17091137.

[36] G. Yang, Y. Wang, M. Sun, P. Xu, C. Wang, K. Huang, H. Jiang, S. Mintova, H. Guo, Is amino-modification of HKUST-1 in PEI mixed-matrix membranes always favorable to CO2 separation?, Microporous and Mesoporous Materials 359 (2023) 112649. https://doi.org/10.1016/j.micromeso.2023.112649.

[37] J. Getzschmann, I. Senkovska, D. Wallacher, M. Tovar, D. Fairen-Jimenez, T. Düren, J.M. Van Baten, R. Krishna, S. Kaskel, Methane storage mechanism in the metal-organic framework Cu3(btc)2: An in situ neutron diffraction study, Microporous and Mesoporous Materials 136 (2010) 50–58. https://doi.org/10.1016/j.micromeso.2010.07.020.

[38] A. Katare, S. Kumar, S. Kundu, S. Sharma, L.M. Kundu, B. Mandal, Mixed Matrix Membranes for Carbon Capture and Sequestration: Challenges and Scope, ACS Omega 8 (2023) 17511–17522. https://doi.org/10.1021/acsomega.3c01666.

[39] M. Dmitrenko, A. Kuzminova, A. Zolotarev, D. Markelov, A. Komolkin, E. Loginova, T. Plisko, K. Burts, A. Bildyukevich, A. Penkova, Modification strategies of polyacrylonitrile ultrafiltration membrane using TiO2 for enhanced antifouling performance in water treatment, Separation and Purification Technology 286 (2022) 120500. https://doi.org/10.1016/j.seppur.2022.120500.

[40] A. Kuzminova, M. Dmitrenko, A. Stepanova, A. Karyakina, A. Selyutin, R. Su, A. Penkova, Novel Mixed-Matrix Pervaporation Membrane Based on Polyether Block Amide Modified with Ho-Based Metal–Organic Framework, Polymers 16 (2024) 3245. https://doi.org/10.3390/polym16233245.

[41] A. Kuzminova, M. Dmitrenko, R. Dubovenko, A. Mikulan, A. Stepanova, M. Puzikova, N. Rakovskaya, A. Mazur, A. Shurukhina, A. Rudakova, A. Emeline, R. Su, A. Penkova, Sustainable Novel Membranes Based on Carboxymethyl Cellulose Modified with ZIF-8 for Isopropanol/Water Pervaporation Separation, Sustainability 17 (2025) 3801. https://doi.org/10.3390/su17093801.

[42] M. Dmitrenko, A. Chepeleva, V. Liamin, A. Mazur, K. Semenov, N. Solovyev, A. Penkova, Novel Mixed Matrix Membranes Based on Polyphenylene Oxide Modified with Graphene Oxide for Enhanced Pervaporation Dehydration of Ethylene Glycol, Polymers 14 (2022) 691. https://doi.org/10.3390/polym14040691.

[43] M. Dmitrenko, O. Mikhailovskaya, R. Dubovenko, A. Kuzminova, D. Myznikov, A. Mazur, K. Semenov, Y. Rusalev, A. Soldatov, S. Ermakov, A. Penkova, Pervaporation Membranes Based on Polyelectrolyte Complex of Sodium Alginate/Polyethyleneimine Modified with Graphene Oxide for Ethanol Dehydration, Polymers 16 (2024) 1206. https://doi.org/10.3390/polym16091206.

[44] A.V. Penkova, M.E. Dmitrenko, S.S. Ermakov, A.M. Toikka, D. Roizard, Novel green PVA-fullerenol mixed matrix supported membranes for separating water-THF mixtures by pervaporation, Environ Sci Pollut Res 25 (2018) 20354–20362. https://doi.org/10.1007/s11356-017-9063-9.

[45] A. Khorsandi-Langol, S.M. Hashemianzadeh, Distinct Understanding of Constant-Volume/Variable-Pressure Experimental Method on CO_2 Capture Using Graphtriyne Membrane through an Atomistic Approach, J. Phys. Chem. C 123 (2019) 15523–15533. https://doi.org/10.1021/acs.jpcc.9b01988.

[46] F. Feng, C.-Z. Liang, J. Wu, M. Weber, C. Maletzko, S. Zhang, T.-S. Chung, Polyphenylsulfone (PPSU)-Based Copolymeric Membranes: Effects of Chemical Structure and Content on Gas Permeation and Separation, Polymers 13 (2021) 2745. https://doi.org/10.3390/polym13162745.

[47] M.J. Frisch, Gaussian 16, Revision A.03, (2016).

[48] W. Humphrey, A. Dalke, K. Schulten, VMD: Visual molecular dynamics, Journal of Molecular Graphics 14 (1996) 33–38. https://doi.org/10.1016/0263-7855(96)00018-5.

[49] C. Adamo, V. Barone, Toward reliable density functional methods without adjustable parameters: The PBE0 model, The Journal of Chemical Physics 110 (1999) 6158–6170. https://doi.org/10.1063/1.478522.

[50] I.O. Putnin, A.A. Sysoeva, A.V. Kovalenko, M.V. Il'in, D.S. Bolotin, Acridine orange as a highly sensitive probe to study the stability of onium salts, New J. Chem. 49 (2025) 9408–9415. https://doi.org/10.1039/D5NJ01326G.

[51] T. Lu, F. Chen, Multiwfn: A multifunctional wavefunction analyzer, Journal of Computational Chemistry 33 (2012) 580–592. https://doi.org/10.1002/jcc.22885.

[52] E.R. Johnson, S. Keinan, P. Mori-Sánchez, J. Contreras-García, A.J. Cohen, W. Yang, Revealing Noncovalent Interactions, Journal of the American Chemical Society 132 (2010) 6498–6506. https://doi.org/10.1021/ja100936w.

[53] M. Dmitrenko, O. Mikhailovskaya, R. Dubovenko, A. Kuzminova, D. Myznikov, A. Mazur, K. Semenov, Y. Rusalev, A. Soldatov, S. Ermakov, A. Penkova, Pervaporation Membranes Based on Polyelectrolyte Complex of Sodium Alginate/Polyethyleneimine Modified with Graphene Oxide for Ethanol Dehydration, Polymers 16 (2024). https://doi.org/10.3390/polym16091206.

[54] B.K. Chen, C.T. Su, M.C. Tseng, S.Y. Tsay, Preparation of polyetherimide nanocomposites with improved thermal, mechanical and dielectric properties, Polymer Bulletin 57 (2006) 671–681. https://doi.org/10.1007/s00289-006-0630-3.

[55] B.K. Chen, J.U. Du, C.W. Hou, The effects of chemical structure on the dielectric properties of polyetherimide and nanocomposites, IEEE Transactions on Dielectrics and Electrical Insulation 15 (2008) 127–133. https://doi.org/10.1109/T-DEI.2008.4446743.

[56] F. Hamidavi, A. Kargari, A. Eliassi, Sorption and permeation study of polyetherimide/hydrophobic silica nanocomposite membrane for effective syngas (H2/CO/CO2) separation, Separation and Purification Technology 279 (2021) 119774. https://doi.org/10.1016/j.seppur.2021.119774.

[57] M. Rezakazemi, A. Ebadi Amooghin, M.M. Montazer-Rahmati, A.F. Ismail, T. Matsuura, State-of-the-art membrane based CO2 separation using mixed matrix membranes (MMMs): An overview on current status and future directions, Progress in Polymer Science 39 (2014) 817–861. https://doi.org/10.1016/j.progpolymsci.2014.01.003.

[58] C.E. Goodyer, A.L. Bunge, Mass transfer through membranes with surface roughness, Journal of Membrane Science 409–410 (2012) 127–136. https://doi.org/10.1016/j.memsci.2012.03.043.

[59] P. Jagódka, K. Matus, A. Łamacz, On the HKUST-1/GO and HKUST-1/rGO Composites: The Impact of Synthesis Method on Physicochemical Properties, Molecules 27 (2022). https://doi.org/10.3390/molecules27207082.

[60] B. Seoane, J. Coronas, I. Gascon, M.E. Benavides, O. Karvan, J. Caro, F. Kapteijn, J. Gascon, Metal-organic framework based mixed matrix membranes: A solution for highly efficient CO2 capture?, Chemical Society Reviews 44 (2015) 2421–2454. https://doi.org/10.1039/c4cs00437j.

[61] R. Naim, A.F. Ismail, Effect of polymer concentration on the structure and performance of PEI hollow fiber membrane contactor for CO2 stripping, Journal of Hazardous Materials 250–251 (2013) 354–361. https://doi.org/10.1016/j.jhazmat.2013.01.083.

[62] R. Naim, A.F. Ismail, T. Matsuura, I.A. Rudaini, S. Abdullah, Polyetherimide hollow fiber membranes for CO2 absorption and stripping in membrane contactor application, RSC Advances 8 (2018) 3556–3563. https://doi.org/10.1039/c7ra12045a.

[63] M.E.A. Safy, M. Amin, R.R. Haikal, B. Elshazly, J. Wang, Y. Wang, C. Wöll, M.H. Alkordi, Probing the Water Stability Limits and Degradation Pathways of Metal–Organic Frameworks, Chemistry – A European Journal 26 (2020) 7109–7117. https://doi.org/10.1002/chem.202000207.

[64] H. Geistlinger, B. Zulfiqar, The Impact of Wettability and Surface Roughness on Fluid Displacement and Capillary Trapping in 2-D and 3-D Porous Media: 1. Wettability-Controlled Phase Transition of Trapping Efficiency in Glass Beads Packs, Water Resources Research 56 (2020) e2019WR026826. https://doi.org/10.1029/2019WR026826.

[65] D.M. Sato, L.M. Guerrini, M.P. De Oliveira, L.R.D.O. Hein, E.C. Botelho, Production and characterization of polyetherimide mats by an electrospinning process, Mater. Res. Express 5 (2018) 115302. https://doi.org/10.1088/2053-1591/aadd85.

[66] C.J. Wijaya, S. Ismadji, H.W. Aparamarta, S. Gunawan, Statistically optimum HKUST-1 synthesized by room temperature coordination modulation method for the adsorption of crystal violet dye, Molecules 26 (2021). https://doi.org/10.3390/molecules26216430.

[67] G. Rabilloud, Adhesives for Electronics, in: Handbook of Adhesives and Surface Preparation, Elsevier, 2011: pp. 259–299. https://doi.org/10.1016/B978-1-4377-4461-3.10012-4.

[68] W. Webo, M.C. Khoathane, W. Mhike, Polymer Composites Reinforced with Cellulosic and Cellulosic-Synthetic Fillers: A Numerical and Experimental Study, International Journal of Engineering Trends and Technology 73 (2025) 1–13. https://doi.org/10.14445/22315381/IJETT-V73I1P101.

[69] K.B. Wiberg, Application of the pople-santry-segal CNDO method to the cyclopropylcarbinyl and cyclobutyl cation and to bicyclobutane, Tetrahedron 24 (1968) 1083–1096. https://doi.org/10.1016/0040-4020(68)88057-3.

[70] C. Trindle, Bond index description of delocalization, Journal of the American Chemical Society 91 (1969) 219–220. https://doi.org/10.1021/ja01029a057.

[71] I. Mayer, P. Salvador, Overlap populations, bond orders and valences for 'fuzzy' atoms, Chemical Physics Letters 383 (2004) 368–375. https://doi.org/10.1016/j.cplett.2003.11.048.

[72] A. Bondi, van der Waals Volumes and Radii, The Journal of Physical Chemistry 68 (1964) 441–451. https://doi.org/10.1021/j100785a001.

[73] I. Mata, I. Alkorta, E. Espinosa, E. Molins, Relationships between interaction energy, intermolecular distance and electron density properties in hydrogen bonded complexes under external electric fields, Chemical Physics Letters 507 (2011) 185–189. https://doi.org/10.1016/j.cplett.2011.03.055.

[74] D.C. Georgiou, P. Butler, E.C. Browne, D.J.D. Wilson, J.L. Dutton, On the Bonding in Bis-pyridine Iodonium Cations, Australian Journal of Chemistry 66 (2013) 1179. https://doi.org/10.1071/CH13202.

[75] Y. Wang, G. Yang, H. Guo, X. Meng, G. Kong, Y. Wang, G. Yang, H. Guo, X. Meng, G. Kong, Preparation of HKUST-1 / PEI mixed-matrix membranes : adsorption-diffusion coupling control of small gas molecules To cite this version : HAL Id : hal-03429763, (2021).

[76] B.D. Bhide, S.A. Stern, A new evaluation of membrane processes for the oxygen-enrichment of air. II. Effects of economic parameters and membrane properties, Journal of Membrane Science 62 (1991) 37–58. https://doi.org/10.1016/0376-7388(91)85003-N.

[77] R. Mahajan, W.J. Koros, Mixed matrix membrane materials with glassy polymers. Part 1, Polymer Engineering and Science 42 (2002) 1420–1431. https://doi.org/10.1002/pen.11041.

[78] R. Lin, B. Villacorta Hernandez, L. Ge, Z. Zhu, Metal organic framework based mixed matrix membranes: an overview on filler/polymer interfaces, J. Mater. Chem. A 6 (2018) 293–312. https://doi.org/10.1039/C7TA07294E.

[79] A.E. Soldatova, R.N. Shamsutdinova, T.V. Plisko, K.S. Burts, A.Yu. Tsegelskaya, D.A. Khanin, K.Z. Monakhova, T.S. Kurkin, A.V. Bildyukevich, A.A. Kuznetsov, Synthesis of Aromatic Polyimides Based on 3,4′-Oxydianiline by One-Pot Polycondensation in Molten Benzoic Acid and Their Application as Membrane Materials for Pervaporation, Materials 15 (2022) 6845. https://doi.org/10.3390/ma15196845.

[80] Y. Wang, L. Jiang, T. Matsuura, T.S. Chung, S.H. Goh, Investigation of the fundamental differences between polyamide-imide (PAI) and polyetherimide (PEI) membranes for isopropanol dehydration via pervaporation, Journal of Membrane Science 318 (2008) 217–226. https://doi.org/10.1016/j.memsci.2008.02.033.

[81] B. Nayak, B.V.R. Kuncharam, Investigation of mixed matrix membranes of graphene and acid-treated graphene fillers in cellulose acetate and polyetherimide polymers for CO_2 separation from biogas, Polymer Engineering & Sci 64 (2024) 6265–6277. https://doi.org/10.1002/pen.26985.

[82] K. Maqsood, A. Jamil, A. Ahmed, B. Sutisna, S. Nunes, M. Ulbricht, Blend membranes comprising polyetherimide and polyvinyl acetate

with improved methane enrichment performance, Chemosphere 321 (2023) 138074. https://doi.org/10.1016/j.chemosphere.2023.138074.

[83] P. Francesco Zito, A. Brunetti, G. Barbieri, Renewable biomethane production from biogas upgrading via membrane separation: Experimental analysis and multistep configuration design, Renewable Energy 200 (2022) 777–787. https://doi.org/10.1016/j.renene.2022.09.124.

Supplementary

The Cartesian coordinates of molecules and their associates are presented in Table S1.

Table S1. The Cartesian coordinates of molecules and their associates.

Atom	X	Y	Z	Atom	X	Y	Z
PEI-I				***PEI-II···BTC-1***			
O	-5.11398	-1.03113	0.160826	**C**	3.439979	-0.32761	0.926816
C	-3.91714	-0.36721	0.060668	**C**	4.558282	-1.15918	0.903753
C	-2.76425	-1.15397	0.176408	**C**	3.367373	0.779856	0.08009
C	-1.55486	-0.50334	0.076745	**H**	4.621172	-2.0177	1.55721
C	-1.46547	0.873244	-0.12658	**H**	2.495381	1.418388	0.104941
C	-2.60231	1.651499	-0.24204	**C**	5.606898	-0.88255	0.024638
C	-3.84081	1.014774	-0.14577	**C**	4.421561	1.053335	-0.7891
C	-0.18121	-1.05165	0.155867	**C**	5.543049	0.222719	-0.82119
N	0.683381	0.047796	-0.00771	**H**	6.353405	0.444408	-1.5017
C	-0.04271	1.248605	-0.18484	**C**	6.7662	-1.78943	0.024644
O	0.446935	2.366447	-0.34729	**O**	6.884477	-2.78386	0.741389
O	0.158239	-2.22256	0.323544	**O**	7.728485	-1.42102	-0.8676
C	2.101073	-0.03785	0.002531	**H**	8.479085	-2.03927	-0.84514
C	2.736535	-1.1044	-0.63602	**C**	4.394342	2.213161	-1.6952
C	4.125389	-1.18756	-0.61411	**O**	5.286943	2.508265	-2.49068
C	4.881634	-0.20657	0.023766	**O**	3.258998	2.956567	-1.57159
C	4.239865	0.859294	0.650853	**H**	3.270278	3.714687	-2.18068
C	2.850975	0.944692	0.651602	**C**	2.305233	-0.58881	1.826429
H	-2.84412	-2.21913	0.33526	**O**	1.256492	0.059711	1.848172
H	-2.53385	2.71863	-0.40135	**O**	2.518513	-1.64448	2.659527
H	-4.75177	1.594537	-0.23133	**H**	1.748612	-1.79813	3.233708
H	2.150138	-1.86743	-1.12443	**O**	-4.27773	5.045591	0.562555
H	4.614761	-2.01934	-1.1023	**C**	-3.90369	3.716317	0.474599
H	5.961198	-0.27221	0.03228	**C**	-4.03049	2.97158	-0.69709
H	2.35348	1.773236	1.131711	**C**	-3.63999	1.636816	-0.70827
H	4.818756	1.626087	1.147427	**C**	-3.11589	1.016107	0.432844
H	-5.88205	-0.44838	0.075512	**C**	-2.99644	1.788451	1.593253
PEI-II				**C**	-3.38759	3.12447	1.620595
O	-4.71646	-1.78764	-0.1214	**C**	-2.6648	-0.44498	0.352011
C	-3.558	-1.03311	-0.11477	**C**	-3.7988	-1.30327	-0.21815
C	-2.50704	-1.2537	-1.00365	**C**	-1.39911	-0.4986	-0.52367
C	-1.37003	-0.45683	-0.93468	**C**	-2.29627	-1.01263	1.735366
C	-1.25135	0.571	0.009072	**C**	-3.58306	-2.30466	-1.17191
C	-2.32008	0.769404	0.889402	**C**	-4.62288	-3.10815	-1.631
C	-3.46373	-0.02275	0.834168	**C**	-5.90798	-2.92329	-1.1374
C	-0.00013	1.454336	-0.00024	**C**	-6.15113	-1.9363	-0.18319
C	1.251557	0.57169	-0.00878	**C**	-5.10294	-1.13971	0.265551

C	-0.07703	2.361598	-1.24147	**O**	-6.90119	-3.74931	-1.63282
C	0.076139	2.36297	1.240008	**H**	-4.43644	3.425587	-1.59417
C	2.319221	0.768375	-0.89083	**H**	-3.7604	1.060574	-1.61749
C	3.462902	-0.02372	-0.83545	**H**	-2.59242	1.352939	2.495775
C	3.558125	-1.03259	0.114953	**H**	-3.29933	3.718043	2.51918
C	2.508461	-1.25111	1.005916	**H**	-0.97598	-1.50612	-0.54663
C	1.371445	-0.45426	0.936923	**H**	-1.6092	-0.18498	-1.54807
O	4.716369	-1.78746	0.121346	**H**	-0.64535	0.167536	-0.10289
H	-2.57047	-2.04466	-1.74235	**H**	-2.05692	-2.07332	1.631007
H	-0.55041	-0.64677	-1.61664	**H**	-3.12935	-0.92493	2.436316
H	-2.27208	1.548442	1.637013	**H**	-1.42112	-0.50432	2.145996
H	-4.28755	0.129211	1.516674	**H**	-2.59281	-2.46707	-1.5743
H	0.749097	3.076396	-1.26205	**H**	-4.45496	-3.8786	-2.36838
H	-0.05975	1.778604	-2.16421	**H**	-7.15203	-1.78461	0.20657
H	-1.011	2.925773	-1.2173	**H**	-5.30378	-0.36416	0.993197
H	1.009479	2.928098	1.214995	**H**	-4.61854	5.384443	-0.27747
H	0.059632	1.781	2.163406	**H**	-7.77034	-3.53709	-1.265
H	-0.75071	3.076948	1.260007	***PEI-II⋯BTC-2***			
H	2.270309	1.545997	-1.63979	**C**	4.150605	-0.12963	-0.22183
H	4.285693	0.126612	-1.51958	**C**	4.986971	-1.22553	-0.02314
H	2.572754	-2.04073	1.745934	**C**	4.68717	1.154106	-0.32069
H	0.552841	-0.64269	1.620429	**H**	4.573571	-2.2209	0.056561
H	-4.70809	-2.46496	-0.81214	**H**	4.026911	1.996145	-0.47498
H	4.708129	-2.4643	0.812562	**C**	6.367186	-1.0362	0.07307
BTC				**C**	6.065031	1.338171	-0.21544
C	0.06969	-1.39048	-2E-06	**C**	6.909639	0.243807	-0.02062
C	-1.17272	-0.75914	-6E-06	**H**	7.976546	0.398502	0.05734
C	1.243798	-0.636	-8E-06	**C**	7.215815	-2.21993	0.275383
H	-2.0854	-1.33831	-0.00001	**O**	6.806848	-3.37872	0.366021
H	2.20172	-1.13681	-1.4E-05	**O**	8.543712	-1.91721	0.356224
C	-1.23906	0.63491	-3E-06	**H**	9.073086	-2.72182	0.489441
C	1.169359	0.755634	0	**C**	6.674455	2.67405	-0.29995
C	-0.07109	1.395203	0.000007	**O**	7.880844	2.90975	-0.21522
H	-0.11633	2.475195	0.000018	**O**	5.758417	3.667805	-0.48452
C	-2.56974	1.26336	-1.6E-05	**H**	6.195518	4.535094	-0.53394
O	-3.63931	0.652915	-7.7E-05	**C**	2.68558	-0.28829	-0.32644
O	-2.51423	2.625768	0.000056	**O**	1.917781	0.655502	-0.55937
H	-3.40835	3.00879	0.000052	**O**	2.271757	-1.55017	-0.13905
C	2.378999	1.593753	0	**H**	1.281405	-1.67137	-0.18092
O	2.385216	2.825242	0.000055	**O**	-9.61768	-1.11249	-1.33587
O	3.531068	0.864387	-7.1E-05	**C**	-8.44464	-0.56211	-0.8549
H	4.309892	1.447129	-7.5E-05	**C**	-7.32344	-0.35039	-1.65604
C	0.19075	-2.85711	0.000013	**C**	-6.17632	0.203907	-1.09905
O	1.254173	-3.47819	0.000028	**C**	-6.11771	0.560726	0.254175
O	-1.0169	-3.49021	0.000018	**C**	-7.25616	0.335713	1.034718

H	-0.90159	-4.45605	0.000037	**C**	-8.41054	-0.22214	0.491556
H_2O				**C**	-4.84425	1.212521	0.799133
O	0	0	0.111188	**C**	-3.63447	0.327678	0.482211
H	0	0.789057	-0.44475	**C**	-4.72246	2.6095	0.164479
H	0	-0.78906	-0.44475	**C**	-4.89369	1.395409	2.326951
iPrOH				**C**	-2.41869	0.843915	0.021475
C	1.204899	-0.76559	-0.10574	**C**	-1.30816	0.028437	-0.18839
H	1.180863	-1.78883	0.273921	**C**	-1.41917	-1.32905	0.069961
H	1.213044	-0.79742	-1.19656	**C**	-2.61178	-1.88002	0.52606
C	-0.00183	0.024334	0.374298	**C**	-3.70778	-1.04878	0.728663
H	0.006423	0.07259	1.471054	**O**	-0.28855	-2.12705	-0.14216
H	2.137964	-0.30651	0.23204	**H**	-7.34129	-0.61845	-2.70599
C	-1.31423	-0.56687	-0.09156	**H**	-5.30441	0.348994	-1.72516
H	-1.33356	-0.60573	-1.18178	**H**	-7.2573	0.593996	2.084274
H	-1.44575	-1.57671	0.30068	**H**	-9.28885	-0.39861	1.09594
H	-2.14522	0.053629	0.242566	**H**	-3.88227	3.166013	0.58581
O	0.026464	1.37142	-0.16276	**H**	-4.59302	2.54723	-0.91745
H	0.841491	1.82643	0.098202	**H**	-5.63429	3.174715	0.364576
PEI-I⋯BTC-1				**H**	-3.95069	1.826913	2.667124
O	4.058657	5.373624	0.024422	**H**	-5.03092	0.44224	2.841238
C	3.609676	4.078735	0.009083	**H**	-5.70063	2.072363	2.617503
C	4.599323	3.085246	0.005757	**H**	-2.31857	1.899729	-0.18402
C	4.165878	1.780171	-0.00837	**H**	-0.36396	0.436002	-0.52565
C	2.808681	1.446578	-0.02203	**H**	-2.68992	-2.94248	0.724926
C	1.827211	2.42379	-0.01846	**H**	-4.63972	-1.47785	1.074231
C	2.249244	3.754996	-0.00273	**H**	-9.57132	-1.31043	-2.28123
C	4.953143	0.528008	-0.01575	**H**	-0.46404	-3.07049	-0.02621
N	4.002404	-0.52175	-0.0327	***PEI-II⋯H_2O-1***			
C	2.698417	-0.01663	-0.03369	**O**	-5.09085	-1.99777	-0.29666
O	1.680408	-0.72604	-0.0472	**C**	-3.97884	-1.17773	-0.25264
O	6.172782	0.386368	-0.00305	**C**	-2.86451	-1.36954	-1.06814
C	4.335877	-1.90434	-0.03978	**C**	-1.77909	-0.50736	-0.96292
C	5.340049	-2.37525	0.806592	**C**	-1.77466	0.558023	-0.0541
C	5.669498	-3.72717	0.790923	**C**	-2.90569	0.727639	0.750844
C	4.991505	-4.60814	-0.04902	**C**	-3.99905	-0.12923	0.657991
C	3.985492	-4.12981	-0.88604	**C**	-0.56881	1.500835	-0.01377
C	3.660018	-2.77702	-0.89302	**C**	0.717223	0.682741	0.140012
H	5.644631	3.356084	0.014878	**C**	-0.57603	2.330645	-1.31046
H	0.772774	2.169637	-0.02888	**C**	-0.63884	2.480268	1.171593
H	1.510051	4.546878	-0.00014	**C**	1.872839	0.937782	-0.60633
H	5.866119	-1.69015	1.454086	**C**	3.047408	0.216921	-0.40298
H	6.45292	-4.09069	1.441515	**C**	3.070037	-0.77442	0.569195
H	5.244998	-5.65951	-0.05128	**C**	1.938086	-1.05648	1.328535
H	2.880287	-2.40437	-1.53971	**C**	0.774462	-0.32728	1.108909
H	3.454332	-4.80759	-1.54011	**O**	4.263646	-1.47605	0.736961

H	3.342992	6.025485	0.025933	**H**	-2.83957	-2.18859	-1.77745
C	-3.1348	0.016443	0.014576	**H**	-0.91003	-0.67462	-1.58694
C	-3.64977	-1.27744	0.053867	**H**	-2.94642	1.534682	1.468119
C	-3.99482	1.114257	-0.0126	**H**	-4.87075	7.46E-05	1.283171
H	-2.98443	-2.12924	0.075114	**H**	0.206412	3.09259	-1.29852
H	-3.58241	2.11257	-0.04393	**H**	-0.43625	1.699395	-2.18984
C	-5.03222	-1.47206	0.065499	**H**	-1.53754	2.837513	-1.40802
C	-5.37407	0.912785	0.000363	**H**	0.265938	3.090169	1.188793
C	-5.89716	-0.3805	0.040724	**H**	-0.7057	1.950862	2.123692
H	-6.96814	-0.5245	0.049478	**H**	-1.4971	3.151432	1.0807
C	-5.53862	-2.85266	0.105042	**H**	1.874531	1.708916	-1.36376
O	-4.83779	-3.8652	0.124534	**H**	3.945256	0.412155	-0.97649
O	-6.90145	-2.91858	0.11785	**H**	1.955697	-1.83959	2.078621
H	-7.2026	-3.84278	0.142615	**H**	-0.11102	-0.55787	1.688495
C	-6.32059	2.038014	-0.0275	**H**	-5.00326	-2.69854	-0.95756
O	-7.5479	1.93208	-0.01773	**H**	4.24151	-2.08092	1.490729
O	-5.70476	3.255566	-0.06641	**O**	6.132133	-0.51443	-1.07757
H	-6.3625	3.971415	-0.08434	**H**	6.29142	-1.19113	-1.74579
C	-1.67883	0.261457	-0.00046	**H**	5.630206	-0.89753	-0.33424
O	-1.18718	1.400647	-0.04005	***PEI-II⋯H₂O-2***			
O	-0.95254	-0.86009	0.032301	**O**	-5.24918	-0.99791	-0.6704
H	0.033409	-0.72479	0.018556	**C**	-3.97442	-0.52225	-0.42051
PEI-I⋯BTC-2				**C**	-2.93158	-0.63937	-1.33851
O	-0.01614	-3.31079	0.053134	**C**	-1.67513	-0.13883	-1.01823
C	1.311181	-2.89832	0.051553	**C**	-1.42404	0.485175	0.210872
C	1.54823	-1.52049	0.026196	**C**	-2.48771	0.585289	1.113447
C	2.874762	-1.13865	0.025628	**C**	-3.75232	0.088353	0.806905
C	3.918741	-2.06195	0.046738	**C**	-0.0343	1.066194	0.481995
C	3.674405	-3.42167	0.073076	**C**	1.043408	-0.00327	0.265365
C	2.342478	-3.83915	0.075071	**C**	0.153789	2.265724	-0.4682
C	3.463065	0.222464	0.002189	**C**	0.104175	1.577382	1.927037
N	4.862136	0.038647	0.012747	**C**	2.318603	0.31868	-0.22064
C	5.199249	-1.33012	0.039553	**C**	3.304545	-0.65475	-0.35108
O	6.33948	-1.79461	0.049204	**C**	3.036014	-1.97006	0.010263
O	2.878939	1.303352	-0.01728	**C**	1.782756	-2.31101	0.513208
C	5.808737	1.097997	-0.00138	**C**	0.80226	-1.33051	0.637898
C	5.582192	2.240881	0.767495	**O**	4.054406	-2.89362	-0.1551
C	6.509136	3.278378	0.742346	**H**	-3.09537	-1.12091	-2.29595
C	7.664746	3.174375	-0.02896	**H**	-0.86601	-0.25033	-1.72923
C	7.887235	2.026383	-0.78642	**H**	-2.34116	1.054105	2.076034
C	6.959571	0.989226	-0.78398	**H**	-4.5724	0.165421	1.506408
H	0.727327	-0.81217	0.010171	**H**	1.104905	2.771218	-0.29774
H	4.48564	-4.13576	0.091121	**H**	0.122308	1.945815	-1.51151
H	2.108697	-4.89669	0.094882	**H**	-0.65585	2.981347	-0.30863
H	4.683772	2.323835	1.359625	**H**	1.119925	1.947059	2.079764

H	6.327342	4.166461	1.3321	**H**	-0.07349	0.777478	2.648697
H	8.38536	3.980849	-0.03986	**H**	-0.59018	2.397125	2.12864
H	7.133965	0.097176	-1.36573	**H**	2.571856	1.334833	-0.49628
H	8.782013	1.936535	-1.3872	**H**	4.286334	-0.40632	-0.72718
H	-0.12046	-4.27241	0.070592	**H**	1.56653	-3.3331	0.803447
C	-5.10773	1.856477	-0.04035	**H**	-0.17169	-1.60752	1.020751
C	-3.84278	1.271066	-0.02577	**H**	-5.32043	-1.40751	-1.54395
C	-6.25386	1.059882	-0.03703	**H**	3.787566	-3.78075	0.123242
H	-2.95068	1.881571	-0.02843	**O**	3.507801	3.37041	-0.9456
H	-7.22902	1.526035	-0.04855	**H**	3.581801	4.124287	-0.34719
C	-3.7253	-0.11936	-0.0078	**H**	3.444816	3.676273	-1.85942
C	-6.12849	-0.32784	-0.01897	***PEI-II···iPrOH-1***			
C	-4.86464	-0.92062	-0.00441	**O**	-6.24745	-2.03116	-0.24169
H	-4.77657	-1.99773	0.00938	**C**	-5.13536	-1.21059	-0.21585
C	-2.37349	-0.70782	0.007258	**C**	-4.00963	-1.43767	-1.00623
O	-1.3342	-0.03434	0.006611	**C**	-2.92591	-0.571	-0.92351
O	-2.37065	-2.05289	0.021826	**C**	-2.93496	0.53374	-0.06275
H	-1.45685	-2.43916	0.03185	**C**	-4.07637	0.73707	0.719738
C	-7.30593	-1.20939	-0.01464	**C**	-5.16808	-0.12413	0.649522
O	-7.26861	-2.44076	0.001274	**C**	-1.73522	1.48561	-0.05565
O	-8.48493	-0.5242	-0.03025	**C**	-0.44344	0.680597	0.116175
H	-9.24095	-1.13584	-0.02697	**C**	-1.75407	2.274827	-1.37705
C	-5.28275	3.317288	-0.05984	**C**	-1.8086	2.50175	1.09833
O	-6.36852	3.899206	-0.07421	**C**	0.683251	0.864256	-0.69207
O	-4.10007	3.99466	-0.06067	**C**	1.860205	0.150341	-0.47848
H	-4.24949	4.955453	-0.07457	**C**	1.915451	-0.76236	0.565995
PEI-I···BTC-3				**C**	0.812954	-0.97116	1.38914
O	-4.24986	4.293949	1.985582	**C**	-0.35427	-0.25211	1.15705
C	-4.15999	3.227904	1.126619	**O**	3.113586	-1.4522	0.748346
C	-3.49512	2.096619	1.617671	**H**	-3.97421	-2.28674	-1.67925
C	-3.39632	1.018051	0.768588	**H**	-2.04864	-0.76457	-1.52839
C	-3.92502	1.03352	-0.5227	**H**	-4.12753	1.574806	1.40067
C	-4.58033	2.148804	-1.00841	**H**	-6.04841	0.031943	1.256324
C	-4.6952	3.256759	-0.16548	**H**	-0.96723	3.032544	-1.398
C	-2.73535	-0.28582	0.975941	**H**	-1.62932	1.61603	-2.23837
N	-2.93581	-1.02022	-0.1826	**H**	-2.71464	2.782827	-1.47832
C	-3.63412	-0.2619	-1.1597	**H**	-0.90748	3.117469	1.093796
O	-3.91279	-0.65193	-2.29016	**H**	-1.87088	2.003035	2.067397
O	-2.11525	-0.66757	1.981468	**H**	-2.67068	3.163823	0.988097
C	-2.41163	-2.32117	-0.40595	**H**	0.656727	1.568842	-1.51095
C	-2.65868	-3.32987	0.524691	**H**	2.729952	0.282941	-1.10845
C	-2.14115	-4.60359	0.30737	**H**	0.857439	-1.68828	2.200813
C	-1.39744	-4.8719	-0.84055	**H**	-1.21778	-0.42953	1.785776
C	-1.16004	-3.85788	-1.76713	**H**	-6.15135	-2.75853	-0.87228
C	-1.6567	-2.57593	-1.55015	**H**	3.061347	-2.11757	1.447926

H	-3.08369	2.096205	2.615922	**O**	4.972574	-0.62794	-1.18137
H	-4.98645	2.166618	-2.01003	**H**	4.431919	-1.06229	-0.49161
H	-5.20026	4.148536	-0.51615	**C**	6.122592	0.018668	-0.59249
H	-3.24089	-3.11371	1.409248	**H**	6.632531	0.47705	-1.44134
H	-2.32581	-5.38567	1.031124	**C**	7.040987	-1.01164	0.048721
H	-1.00378	-5.86498	-1.01112	**C**	5.693985	1.10222	0.386695
H	-1.46623	-1.77976	-2.25407	**H**	5.037262	1.819624	-0.10664
H	-0.58056	-4.06125	-2.65727	**H**	5.14862	0.660763	1.224907
H	-4.70268	5.058165	1.601143	**H**	6.558378	1.638213	0.785002
C	2.197542	0.149439	0.305949	**H**	6.544096	-1.4838	0.90145
C	3.188783	-0.23368	1.206478	**H**	7.963538	-0.5513	0.409221
C	2.537448	0.806784	-0.87671	**H**	7.295527	-1.78747	-0.67378
H	2.926463	-0.73352	2.128345	***PEI-II···iPrOH-2***			
H	1.756987	1.105549	-1.5621	**O**	-2.09915	4.226586	0.169879
C	4.528247	0.033648	0.915667	**C**	-1.41905	3.02151	0.139439
C	3.875924	1.072512	-1.16017	**C**	-0.26193	2.788467	0.878488
C	4.875529	0.682759	-0.26735	**C**	0.372589	1.552522	0.791411
H	5.910628	0.890569	-0.49873	**C**	-0.12505	0.529068	-0.02327
C	5.545908	-0.38027	1.893609	**C**	-1.29596	0.785726	-0.74798
O	5.311099	-0.92076	2.975229	**C**	-1.93692	2.019343	-0.67346
O	6.819011	-0.10282	1.488179	**C**	0.560065	-0.842	-0.03878
H	7.463714	-0.38388	2.159701	**C**	2.079771	-0.66588	-0.00959
C	4.281254	1.764277	-2.39308	**C**	0.041163	-1.63447	1.17458
O	5.443726	2.005886	-2.72146	**C**	0.199751	-1.64585	-1.3037
O	3.222636	2.130851	-3.17226	**C**	2.906188	-1.28878	0.93116
H	3.528442	2.578287	-3.9798	**C**	4.290583	-1.13916	0.897135
C	0.769794	-0.10981	0.575161	**C**	4.875445	-0.3566	-0.09013
O	-0.14098	0.243826	-0.18898	**C**	4.075883	0.280014	-1.03853
O	0.553235	-0.76188	1.730337	**C**	2.695585	0.122306	-0.99079
H	-0.41184	-0.89147	1.916223	**O**	6.254282	-0.24354	-0.07507
PEI-I···H₂O-1				**H**	0.149012	3.564658	1.514444
O	5.332979	-0.86023	-0.34856	**H**	1.278968	1.384916	1.359104
C	4.092727	-0.32246	-0.11905	**H**	-1.7306	0.012287	-1.36495
C	3.001957	-1.17244	-0.34625	**H**	-2.83397	2.222221	-1.24154
C	1.749244	-0.64912	-0.12084	**H**	0.465903	-2.64158	1.197777
C	1.558517	0.66361	0.311359	**H**	0.278848	-1.12941	2.113414
C	2.633052	1.503579	0.537214	**H**	-1.04284	-1.72724	1.091936
C	3.914264	0.995306	0.316569	**H**	0.77299	-2.57531	-1.31234
C	0.419125	-1.2828	-0.27172	**H**	0.444687	-1.08997	-2.21093
N	-0.52264	-0.29106	0.084682	**H**	-0.86291	-1.89406	-1.31428
C	0.114119	0.904146	0.449304	**H**	2.475362	-1.90189	1.709816
O	-0.45063	1.941175	0.816079	**H**	4.927068	-1.62039	1.625861
O	0.156249	-2.43024	-0.62306	**H**	4.524841	0.8979	-1.80802
C	-1.93153	-0.49167	0.069273	**H**	2.080993	0.634118	-1.7209
C	-2.45962	-1.65508	0.630589	**H**	-1.67623	4.867623	0.758353

C	-3.83457	-1.86572	0.604783	**H**	6.5821	0.31115	-0.79677
C	-4.68029	-0.91445	0.03762	**O**	-3.24422	-1.94552	-0.61601
C	-4.14284	0.247404	-0.51213	**H**	-3.52935	-2.86054	-0.76958
C	-2.76705	0.464273	-0.50957	**C**	-4.29623	-1.19631	0.057028
H	3.161645	-2.18579	-0.68355	**H**	-3.84645	-0.21417	0.199979
H	2.486148	2.52119	0.871214	**C**	-4.61106	-1.81964	1.405974
H	4.778734	1.626456	0.482011	**C**	-5.51582	-1.08238	-0.84155
H	-1.80035	-2.3919	1.064726	**H**	-5.23594	-0.6651	-1.80916
H	-4.24257	-2.77175	1.03162	**H**	-5.96688	-2.06579	-1.00676
H	-5.74929	-1.07902	0.022353	**H**	-6.27375	-0.43834	-0.39119
H	-2.36583	1.374105	-0.93631	**H**	-5.03527	-2.82071	1.279137
H	-4.79232	0.988935	-0.95742	**H**	-5.33812	-1.21673	1.953704
H	6.056444	-0.23775	-0.18741	**H**	-3.70573	-1.9011	2.007842
O	-1.99641	3.657495	-0.76054	***BTC⋯H₂O-1***			
H	-2.80401	3.950917	-0.3213	**O**	-5.29734	-0.09212	-5.2E-06
H	-1.41018	3.228937	-0.11308	**H**	-4.87181	0.786218	-3.3E-05
PEI-I⋯H₂O-2				**H**	-6.25736	-0.09034	-0.002
O	-5.21495	-1.20886	-0.04024	**C**	1.227172	1.181671	-7.2E-05
C	-4.07421	-0.44887	-0.02004	**C**	-0.16596	1.229031	-7.3E-05
C	-2.86544	-1.15152	-0.11124	**C**	1.890779	-0.04631	-5.9E-05
C	-1.70982	-0.40378	-0.09576	**H**	-0.68709	2.175752	-8.8E-05
C	-1.72343	0.988143	0.009976	**H**	2.971406	-0.07025	-2.9E-05
C	-2.91547	1.682148	0.101295	**C**	-0.89742	0.040982	2.66E-07
C	-4.10174	0.946298	0.084684	**C**	1.153253	-1.22866	-7.1E-05
C	-0.30071	-0.84767	-0.16663	**C**	-0.24222	-1.1885	-2.2E-05
N	0.476341	0.315318	-0.11616	**H**	-0.80852	-2.10935	2.03E-05
C	-0.33369	1.473402	0.002094	**C**	-2.36939	0.11927	0.000154
O	0.085627	2.626039	0.083643	**O**	-2.98676	1.204144	4.57E-05
O	0.128821	-2.0021	-0.25315	**O**	-2.98307	-1.06854	0.000431
C	1.894551	0.333718	-0.17268	**H**	-3.98775	-0.96236	0.000391
C	2.553703	-0.40897	-1.15354	**C**	1.808477	-2.54583	-8.7E-05
C	3.945669	-0.41158	-1.19193	**O**	1.221861	-3.62874	-0.00018
C	4.675268	0.33836	-0.26993	**O**	3.170092	-2.46321	4.56E-05
C	4.007133	1.090928	0.694862	**H**	3.570118	-3.3496	6.06E-05
C	2.616588	1.086218	0.752984	**C**	2.042004	2.406231	6.29E-06
H	-2.86518	-2.22866	-0.18829	**O**	3.273502	2.437318	0.000301
H	-2.92887	2.759995	0.184023	**O**	1.292689	3.546021	-0.00024
H	-5.0531	1.459213	0.154657	**H**	1.863089	4.333686	-0.00014
H	1.983275	-0.98645	-1.86648	***BTC⋯H₂O-2***			
H	4.457163	-0.99351	-1.94627	**O**	-4.23451	-0.06108	0.238289
H	5.756068	0.337987	-0.30507	**H**	-4.64172	-0.32257	-0.59614
H	2.094683	1.66246	1.50195	**H**	-3.87662	0.841584	0.170173
H	4.567584	1.675499	1.4111	**C**	1.760511	0.187368	0.000181
H	-6.02628	-0.68594	0.031303	**C**	1.24086	-1.10517	0.000732
O	2.476083	-2.6727	1.367766	**C**	0.903131	1.28636	-0.00917

H	3.163374	-2.10217	1.002658	**H**	1.897134	-1.96413	0.009114
H	1.701882	-2.64556	0.784469	**H**	1.317538	2.284617	-0.01172
PEI-I⋯H$_2$O-3				**C**	-0.14136	-1.29529	-0.00885
O	-4.84091	-0.01745	0.026016	**C**	-0.4782	1.089212	-0.01255
C	-3.53714	0.447591	-0.0179	**C**	-1.01215	-0.20497	-0.00811
C	-2.52842	-0.51866	0.076114	**H**	-2.08753	-0.3655	0.021773
C	-1.23274	-0.05103	0.017557	**C**	-0.63603	-2.68331	-0.01452
C	-0.93351	1.304029	-0.11976	**O**	0.077283	-3.68246	0.094487
C	-1.93378	2.25327	-0.20853	**O**	-1.98366	-2.76696	-0.1674
C	-3.25644	1.808639	-0.15788	**H**	-2.28526	-3.69064	-0.12897
C	0.043531	-0.80194	0.081391	**C**	-1.3882	2.242445	-0.02862
N	1.065942	0.164605	-0.01847	**O**	-2.62376	2.195374	-0.07276
C	0.531412	1.464862	-0.14397	**O**	-0.74145	3.436351	0.000337
O	1.181503	2.505579	-0.24656	**H**	-1.37219	4.17695	-0.01064
O	0.206591	-2.01586	0.18802	**C**	3.209736	0.441027	0.00874
C	2.45485	-0.13257	0.00253	**O**	3.731414	1.556838	0.006407
C	2.936599	-1.24898	-0.68335	**O**	3.949423	-0.7035	0.019564
C	4.297246	-1.5387	-0.6512	**H**	4.900958	-0.50277	0.027976
C	5.178744	-0.71379	0.044164	***BTC⋯iPrOH-1***			
C	4.690712	0.403261	0.718839	**O**	3.288084	-0.59063	0.81398
C	3.330002	0.694072	0.709406	**H**	2.806065	-1.42168	0.644937
H	-2.78535	-1.56429	0.201721	**C**	-0.57756	1.233081	0.124807
H	-1.69971	3.303277	-0.3147	**C**	0.130464	0.032736	0.199106
H	-4.06821	2.522497	-0.22774	**C**	-1.96845	1.235516	0.011168
H	2.252588	-1.89168	-1.21589	**H**	1.210236	0.042008	0.323838
H	4.666744	-2.40914	-1.17601	**H**	-2.49757	2.176989	-0.03569
H	6.236344	-0.93969	0.060608	**C**	-0.57499	-1.17517	0.138658
H	2.951936	1.562263	1.226946	**C**	-2.65992	0.027645	-0.04145
H	5.367645	1.049677	1.260641	**C**	-1.9651	-1.17917	0.018455
H	-5.50213	0.688623	0.024902	**H**	-2.5114	-2.11064	-0.02771
O	-4.70097	-2.79126	0.34262	**C**	0.163047	-2.44452	0.191299
H	-5.00341	-1.86941	0.273804	**O**	1.39185	-2.57157	0.257248
H	-4.89417	-3.2728	-0.47031	**O**	-0.64479	-3.5357	0.14939
PEI-I⋯iPrOH-1				**H**	-0.12539	-4.35756	0.184436
O	5.918387	-0.79886	0.290592	**C**	-4.12533	-0.02288	-0.16319
C	4.562994	-0.80025	0.081885	**O**	-4.79429	-1.05571	-0.21618
C	3.901424	0.4106	0.325955	**O**	-4.69701	1.213131	-0.21443
C	2.540887	0.428238	0.119184	**H**	-5.66408	1.146388	-0.29244
C	1.839847	-0.69918	-0.30941	**C**	0.098246	2.541628	0.162383
C	2.49026	-1.89477	-0.55135	**O**	-0.48033	3.628365	0.21388
C	3.871034	-1.93698	-0.35058	**O**	1.45464	2.44691	0.117744
C	1.572737	1.537034	0.285225	**H**	1.868104	3.325596	0.172003
N	0.311641	1.002549	-0.06149	**C**	4.321316	-0.36264	-0.17146
C	0.417193	-0.34609	-0.42954	**H**	5.038991	-1.19276	-0.13589
O	-0.51677	-1.07469	-0.78663	**C**	5.014859	0.91634	0.245731

O	1.79089	2.693311	0.638916	**C**	3.723712	-0.27594	-1.56802
C	-0.89955	1.750803	-0.04405	**H**	3.192613	-1.19626	-1.82205
C	-0.92279	3.018451	-0.62689	**H**	3.017769	0.556005	-1.61325
C	-2.09919	3.760591	-0.60708	**H**	4.501237	-0.11563	-2.31825
C	-3.25061	3.235568	-0.02324	**H**	4.292171	1.733822	0.241645
C	-3.21736	1.966331	0.549816	**H**	5.832577	1.159287	-0.43539
C	-2.04262	1.217982	0.552009	**H**	5.411618	0.81632	1.255796
H	4.454486	1.276048	0.660199	***BTC···iPrOH-2***			
H	1.947166	-2.76878	-0.88294	**O**	-4.0976	-0.30907	-0.19773
H	4.412543	-2.8575	-0.53093	**H**	-3.73122	0.597438	-0.17436
H	-0.02704	3.422469	-1.07508	**C**	2.413308	1.210058	0.006221
H	-2.11489	4.745808	-1.0526	**C**	1.019809	1.215604	-0.03135
H	-4.1656	3.812505	-0.01417	**C**	3.11327	0.00253	0.020686
H	-2.03885	0.231208	0.995575	**H**	0.470402	2.146146	-0.04309
H	-4.10527	1.552386	1.008309	**H**	4.19372	0.010921	0.049708
H	6.333524	-1.65566	0.116339	**C**	0.324328	0.006445	-0.05449
O	-2.49836	-1.97898	0.970944	**C**	2.411681	-1.20127	-0.00255
H	-1.86733	-1.82755	0.241559	**C**	1.016033	-1.2027	-0.04031
C	-3.65954	-2.69998	0.497038	**H**	0.477515	-2.13987	-0.05871
H	-4.30254	-2.77034	1.375709	**C**	-1.14956	0.041224	-0.09426
C	-3.25962	-4.09723	0.04694	**O**	-1.79919	1.105781	-0.10802
C	-4.37153	-1.91856	-0.59719	**O**	-1.72657	-1.16504	-0.11459
H	-4.61223	-0.91213	-0.25301	**H**	-2.73578	-1.08645	-0.14273
H	-3.73175	-1.83104	-1.47981	**C**	3.105867	-2.49808	0.011671
H	-5.29701	-2.41598	-0.89583	**O**	2.55263	-3.59836	-0.00569
H	-2.60326	-4.04	-0.8265	**O**	4.464116	-2.37494	0.047229
H	-4.13425	-4.69214	-0.22633	**H**	4.889902	-3.2492	0.055539
H	-2.72378	-4.60866	0.846981	**C**	3.190659	2.458351	0.031564
PEI-I···iPrOH-2				**O**	4.420287	2.526634	0.064557
O	5.082904	-1.55991	-0.6442	**O**	2.40789	3.575433	0.015073
C	3.892009	-1.12975	-0.11388	**H**	2.954612	4.379519	0.032147
C	2.730852	-1.6266	-0.71773	**C**	-5.52879	-0.39985	0.032777
C	1.529479	-1.20536	-0.19403	**H**	-5.73166	-1.46895	-0.03324
C	1.454888	-0.32697	0.883012	**C**	-6.27235	0.335115	-1.0685
C	2.598696	0.164843	1.482777	**C**	-5.86569	0.106584	1.424661
C	3.830456	-0.24696	0.970795	**H**	-5.2863	-0.42926	2.176664
C	0.152486	-1.5502	-0.60721	**H**	-5.63978	1.172797	1.509407
N	-0.70634	-0.86631	0.279987	**H**	-6.92696	-0.03084	1.639911
C	0.039239	-0.07779	1.187734	**H**	-6.05643	1.406048	-1.02761
O	-0.4286	0.654313	2.063299	**H**	-7.35084	0.205077	-0.96092
O	-0.1926	-2.29322	-1.52536	**H**	-5.97111	-0.04088	-2.0461
C	-2.12302	-0.89097	0.201458	***BTC···iPrOH-3***			
C	-2.77668	-2.03934	-0.25717	**O**	3.273057	-0.5062	0.744483
C	-4.16417	-2.04997	-0.35622	**H**	2.76602	-1.29482	0.483466
C	-4.91276	-0.93403	0.011017	**C**	-2.70109	0.054314	-0.07348

C	-4.25859	0.201173	0.481823	**C**	-2.04581	-1.17072	0.008415
C	-2.8697	0.233844	0.573709	**C**	-1.97323	1.243599	-0.02455
H	2.798032	-2.30564	-1.55452	**H**	-2.60318	-2.09593	-0.03174
H	2.541008	0.846134	2.320534	**H**	-2.49049	2.190276	-0.09202
H	4.747863	0.118212	1.416186	**C**	-0.65527	-1.20821	0.145138
H	-2.20435	-2.90276	-0.55532	**C**	-0.58719	1.200129	0.109349
H	-4.65976	-2.94054	-0.71894	**C**	0.081124	-0.02381	0.205213
H	-5.99128	-0.9515	-0.06295	**H**	1.155558	-0.0271	0.35914
H	-2.37373	1.098663	0.98608	**C**	-0.03839	-2.541	0.215847
H	-4.82786	1.07021	0.783681	**O**	-0.656	-3.60387	0.249841
H	5.855462	-1.18394	-0.19929	**O**	1.336781	-2.53495	0.224709
O	-0.2252	1.841237	-1.00226	**H**	1.668387	-3.44839	0.286103
H	-1.17175	1.62655	-0.98478	**C**	0.210508	2.437758	0.131038
C	0.029594	3.120051	-0.35754	**O**	1.439539	2.49417	0.095089
H	-0.1231	3.000968	0.721454	**O**	-0.56083	3.561655	0.182144
C	-0.91058	4.18729	-0.8936	**H**	-0.00793	4.361751	0.18504
C	1.484996	3.430572	-0.63374	**C**	-4.16302	0.141366	-0.21683
H	2.117163	2.613274	-0.28718	**O**	-4.80298	1.190141	-0.29923
H	1.640806	3.552091	-1.70697	**O**	-4.76707	-1.08012	-0.2528
H	1.785669	4.3492	-0.12635	**H**	-5.73081	-0.98896	-0.34614
H	-0.78202	4.28918	-1.97289	**C**	3.958084	0.087672	-0.38901
H	-0.70876	5.15335	-0.42599	**H**	3.213574	0.423337	-1.12178
H	-1.95427	3.932336	-0.69188	**C**	4.886486	-0.9302	-1.03282
PEI-I⋯iPrOH-3				**C**	4.688067	1.293763	0.157672
O	3.697614	1.554628	-0.30137	**H**	3.971948	1.98279	0.602144
C	2.325709	1.656787	-0.14525	**H**	5.398847	0.978068	0.923447
C	1.588595	0.480162	-0.32615	**H**	5.230232	1.810282	-0.63683
C	0.224222	0.586839	-0.15885	**H**	5.615902	-1.27991	-0.29979
C	-0.39681	1.792806	0.164899	**H**	5.422941	-0.49221	-1.87706
C	0.335832	2.951319	0.339392	**H**	4.327354	-1.79378	-1.40371
C	1.720946	2.87288	0.181214	***H_2O⋯iPrOH-1***			
C	-0.82252	-0.45634	-0.27102	**O**	-2.74447	-0.05121	0.096762
N	-2.04605	0.193786	-0.00652	**H**	-3.31803	-0.48415	0.739044
C	-1.84926	1.564741	0.266158	**H**	-3.23841	0.215688	-0.68733
O	-2.73223	2.382151	0.528052	**C**	0.59574	1.426414	-0.11192
O	-0.6815	-1.6501	-0.52947	**H**	1.308658	2.088577	0.384901
C	-3.31271	-0.44897	-0.01143	**H**	0.75042	1.493512	-1.19095
C	-3.44634	-1.72421	0.540733	**C**	0.773664	-0.01741	0.338197
C	-4.68838	-2.35143	0.524833	**H**	0.608165	-0.07177	1.424227
C	-5.79736	-1.70847	-0.02093	**H**	-0.41345	1.777399	0.115168
C	-5.6571	-0.4323	-0.56207	**C**	2.153191	-0.55744	0.022977
C	-4.41689	0.198662	-0.56851	**H**	2.326676	-0.51012	-1.05364
H	2.090222	-0.44385	-0.58958	**H**	2.927893	0.019521	0.532147
H	-0.14704	3.885302	0.590624	**H**	2.225375	-1.60005	0.332665
H	2.329383	3.759457	0.312749	**O**	-0.15941	-0.87894	-0.33766

H	-2.58569	-2.2248	0.956913	**H**	-1.0818	-0.59678	-0.16461
H	-4.78729	-3.34292	0.945309	***H2O···iPrOH-2***			
H	-6.76199	-2.19767	-0.02494	**O**	-2.71635	-0.06605	-0.14578
H	-4.30868	1.189508	-0.98207	**H**	-3.16462	0.126624	0.685852
H	-6.51255	0.07487	-0.98711	**H**	-1.84473	-0.47762	0.029005
H	4.158018	2.401258	-0.21521	**C**	2.178903	-0.29618	0.052366
O	4.231446	-1.13675	-0.95237	**H**	2.869536	0.438414	-0.36543
H	4.31676	-0.18002	-0.77931	**H**	2.263063	-0.27377	1.140031
C	5.030154	-1.9056	-0.02227	**C**	0.75247	0.016076	-0.3608
H	4.824283	-2.94108	-0.29533	**H**	0.656601	-0.04187	-1.45074
C	4.578356	-1.65762	1.409282	**H**	2.490739	-1.28319	-0.29958
C	6.508612	-1.61274	-0.22668	**C**	0.268191	1.366464	0.119492
H	6.780155	-1.76599	-1.27127	**H**	0.376736	1.43586	1.203524
H	6.732781	-0.57541	0.0399	**H**	0.851219	2.16508	-0.34145
H	7.129441	-2.26069	0.395596	**H**	-0.78307	1.496577	-0.13688
H	4.740674	-0.61134	1.683435	**O**	-0.15893	-0.96353	0.230816
H	5.134884	-2.28196	2.111368	**H**	0.089406	-1.86769	-0.01099
H	3.515964	-1.8797	1.515693				

Table S2. Change in thermodynamic potentials (kJ/mol) during the formation of hypothetical associates.

PBE0/6-31G			**ΔH**	**ΔG**	**ΔH_{max}**	**ΔG_{min}**
PEI-I	**BTC**	1	-59.17	-17.14	-59.2	-17.1
		2	-42.52	-2.58		
		3	-43.72	-3.56		
	H_2O	1	-30.63	4.36	-30.6	4.4
		2	-23.83	7.58		
		3	-25.78	9.38		
	iPrOH	1	-28.63	9.65	-28.6	9.7
		2	-13.39	23.62		
		3	-24.55	13.33		
PEI-II	**BTC**	1	-1.55	23.59	-51.7	-12.2
		2	-51.65	-12.21		
	H_2O	1	-30.79	3.92	-30.8	3.9
		2	-8.41	13.54		
	iPrOH	1	-29.41	8.62	-29.4	8.6
		2	-11.69	19.93		
BTC	**H_2O**	1	-74.88	-36.97	-74.9	-37.0
		2	-29.42	5.51		
	iPrOH	1	-30.44	10.23	-72.8	-32.6
		2	-72.82	-32.59		
		3	-19.70	19.68		
H_2O	**iPrOH**	1	-32.68	-2.59	-38.1	-2.6
		2	-38.10	-2.17		

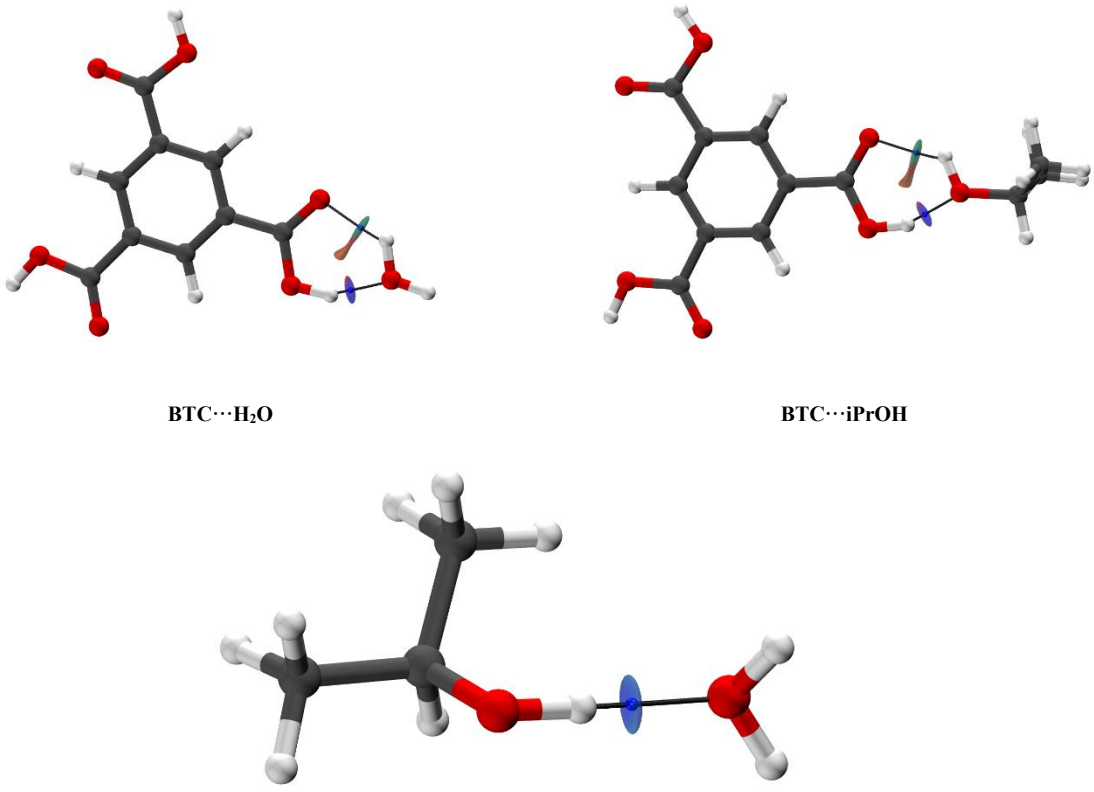


Fig. S1 The NCIplot index isosurfaces and QTAIM distribution of BCPs (blue spheres), as well as bond paths for the associates with components of the feed and BTC.

Table S3. Electron density ρ(r) (e/bohr^3), Laplacian $\nabla^2\rho(r)$ (e/bohr^5), potential energy density V(r) (Hartree), Lagrangian kinetic energy G(r) (Hartree) at the bond CP (3, −1), corresponding to different H-interactions. ^{1}E, ^{2}E, ^{3}E, ^{4}E (kJ/mol) are values of interaction energy.

PBE0/6-31G										
Associate		**Interaction**	**ρ(r)**	**G(r)**	**V(r)**	**$\nabla^2\rho(r)$**	**^{1}E**	**^{2}E**	**^{3}E**	**^{4}E**
PEI-I	BTC	H///O(CO*OH)	0.019	0.016	-0.016	0.068	2.8	2.1	-6.8	16.4
		O///H(COOH)	0.046	0.045	-0.045	0.182	10.4	10.2	-15.0	47.8
	H_2O	H///O	0.014	0.011	-0.011	0.047	1.5	0.8	-5.5	10.5
		O///H	0.029	0.028	-0.028	0.116	5.7	5.5	-10.2	29.6
	iPrOH	O///H(OH)	0.030	0.029	-0.028	0.115	5.8	5.5	-10.2	29.4
		H///O	0.015	0.012	-0.012	0.051	1.7	1.1	-5.8	11.8
PEI-II	BTC	H(CH3)///O(CO*OH)	0.005	0.004	-0.003	0.020	-1.1	-1.3	-3.2	3.0
		H(CH3)*///O(CO*OH)	0.005	0.004	-0.003	0.021	-1.0	-1.2	-3.3	3.5
	H_2O	H(CH3)///O	0.009	0.007	-0.006	0.032	0.1	-0.4	-4.2	6.5
		H(CH)///O	0.014	0.012	-0.012	0.051	1.4	1.0	-5.6	11.8
	iPrOH	H(CH3)///O	0.005	0.004	-0.003	0.021	-1.0	-1.2	-3.3	3.4
		H(CH3)*///O	0.009	0.008	-0.007	0.035	0.2	-0.2	-4.3	7.3
		H(CH)///O	0.007	0.007	-0.005	0.031	-0.3	-0.6	-3.9	6.3
PEI-II(OH)	BTC	O///H(COOH)	0.051	0.049	-0.051	0.186	11.8	11.1	-16.6	48.9
		H(CH)///O(CO*OH)	0.013	0.011	-0.010	0.048	1.3	0.7	-5.3	10.9
	H_2O	O///H	0.034	0.032	-0.033	0.125	6.9	6.4	-11.4	32.2

		H(CH)///O	0.006	0.010	-0.010	0.044	-0.7	0.4	-5.0	9.7
	iPrOH	O///H(OH)	0.032	0.030	-0.031	0.119	6.5	6.0	-11.0	30.6
		H(CH)///O	0.011	0.009	-0.008	0.040	0.6	0.1	-4.7	8.6
		O///H(CH3)	0.004	0.003	-0.002	0.017	-1.3	-1.5	-3.0	2.3
BTC	H_2O	O(CO*OH)///H	0.029	0.026	-0.027	0.102	5.7	4.9	-9.9	25.9
		H(COOH)///O	0.060	0.058	-0.062	0.212	14.2	13.6	-19.7	56.3
	iPrOH	O(CO*OH)///H	0.026	0.023	-0.024	0.090	4.7	4.0	-9.0	22.4
		H(COOH)///O	0.061	0.057	-0.063	0.207	14.5	13.4	-19.7	55.0
H_2O	iPrOH	O///H(OH)	0.040	0.038	-0.040	0.144	8.6	8.0	-13.3	37.5

**[1]E, [2]E, [3]E, [4]E values of interaction energy in case of correlation with 1 - electron density ρ(r), 2 - Lagrangian kinetic energy G(r), 3 - potential energy density V(r), and 4 - Laplacian $\nabla^2\rho(r)$*[1].

Reference

[1] Mata, I.; Alkorta, I.; Espinosa, E.; Molins, E. Relationships between Interaction Energy, Intermolecular Distance and Electron Density Properties in Hydrogen Bonded Complexes under External Electric Fields. *Chem. Phys. Lett.*, **2011**, *507* (1–3), 185–189. https://doi.org/10.1016/j.cplett.2011.03.055.